TRIUMF

Canada's national laboratory
for particle and nuclear physics
and accelerator-based science

Decay and in-beam electron spectroscopy at TRIUMF

Adam Garnsworthy
ARIEL Principal Scientist and TRIUMF Research Scientist

Shape coexistence and electric monopole transitions in atomic nuclei
ESNT Workshop

23-27th October 2017

Outline

- A microscopic model for *E0* transition matrix elements
- First measurement of 2-2 *E0* strengths in spherical nuclei – ^{58,60,62}Ni at ANU
- Shape coexistence studies at TRIUMF-ISAC using gamma-ray and electron spectroscopy
- Questions and observations

RAPID COMMUNICATIONS

PHYSICAL REVIEW C **95**, 011301(R) (2017)

Microscopic method for $E0$ transition matrix elements

B. A. Brown,[1] A. B. Garnsworthy,[2] T. Kibédi,[3] and A. E. Stuchbery[3]

[1] *Department of Physics and Astronomy and National Superconducting Cyclotron Laboratory Michigan State University, East Lansing, Michigan 48824-1321, USA*

[2] *Physical Sciences Division, TRIUMF, 4004 Wesbrook Mall, Vancouver, British Columbia, Canada V6T 2A3*

[3] *Department of Nuclear Physics, Research School of Physics and Engineering, Australian National University, Canberra, Australian Capital Territory 2601, Australia*

(Received 7 April 2016; revised manuscript received 28 October 2016; published 13 January 2017)

Microscopic model for *E0* transition matrix elements.
B.A. Brown *et al.*, PRC 95, 011301(R) (2017).

A theoretical model for *E0* matrix elements based on a combination of configuration interaction (CI) results in a spherical basis for orbital occupations and radii, together with energy-density functional (EDF) calculations for the monopole core polarization.

This core polarization is caused by the change in the nodal structure of the radial wave functions for the orbitals that participate in the valence transition. The core polarization is not proportional to the valence *E0* matrix element.

This method is a generalization of the two-level model and makes connections to isomer and isotope shifts via a common EDF approach.

Microscopic model for *E0* transition matrix elements

Example of ^{90}Zr

Two configurations dominate:

$$|a\rangle = |C_a,(1p_{1/2})^2\rangle \qquad |b\rangle = |C_b,(0g_{9/2})^2\rangle$$

where *C* is ^{88}Sr core.

Radial densities are given by (q=p for proton, q=n for neutron):

$$\rho_{qx}(r) = \sum_k O_{qxk}\, \psi^2_{qxk}(r)$$

where $x = a/b$ and $k = (n,l,j)$ are the quantum numbers for the spherical single-particle wave functions, $\psi_{qxk}(r)[Y^{(l)}(\check{r}) \otimes \chi^{(s)}]^{(j)}$. The *O* are the orbital occupations.

Simplest model: radial wavefunctions depend only on *k*.
EDF model: also depend on a and b – different self-consistent potentials and different radial wavefunctions in the core

Microscopic model for *E0* transition matrix elements

Example of ^{90}Zr

Matrix element of *E0* operator:

$$\int \rho_{px} r^2 \, d\tau = \langle x | r^2 | x \rangle_p = \sum_k O_{pxk} \langle pxk | r^2 | pxk \rangle$$

Two states that mix, here maximal mixing…

$$|0_1^+\rangle = \alpha |a\rangle + \beta |b\rangle \qquad |0_2^+\rangle = \beta |a\rangle - \alpha |b\rangle$$

$$\begin{aligned}\langle 0_1^+ | r^2 | 0_1^+ \rangle = \langle 0_2^+ | r^2 | 0_2^+ \rangle &= \tfrac{1}{2}[\langle b | r^2 | b \rangle + \langle a | r^2 | a \rangle] \\ &= \tfrac{1}{2}\langle C_b | r^2 | C_b \rangle + \tfrac{1}{2}\langle C_a | r^2 | C_a \rangle \\ &\quad + \langle 0g_{9/2} | r^2 | 0g_{9/2} \rangle + \langle 1p_{1/2} | r^2 | 1p_{1/2} \rangle\end{aligned}$$

$$\begin{aligned}\langle 0_1^+ | r^2 | 0_2^+ \rangle &= \tfrac{1}{2}[\langle b | r^2 | b \rangle - \langle a | r^2 | a \rangle] \\ &= \tfrac{1}{2}\langle C_b | r^2 | C_b \rangle - \tfrac{1}{2}\langle C_a | r^2 | C_a \rangle \\ &\quad + \langle 0g_{9/2} | r^2 | 0g_{9/2} \rangle - \langle 1p_{1/2} | r^2 | 1p_{1/2} \rangle\end{aligned}$$

Microscopic model for *E0* transition matrix elements

$$|a\rangle = |C_a, (1p_{1/2})^2\rangle \quad |b\rangle = |C_b, (0g_{9/2})^2\rangle$$ where C is ^{88}Sr core.

Example of ^{90}Zr, Experimental $<0_1^+|r^2|0_2^+>_{ch} = 1.70(3)\ fm^2$

Harmonic Oscillator (HO), core terms all cancel:

$$\langle 0_1^+|r^2|0_2^+\rangle = \frac{11}{2}b^2 - \frac{9}{2}b^2 = b^2$$

where $b^2 = \frac{\hbar}{m\omega}$. With $\hbar\omega = 45\mathrm{A}^{-1/3} - 25\mathrm{A}^{-2/3}$, $b^2 = 4.71\ \mathrm{fm}^2$

Consider finite charge and relativistic contributions: 5.32fm^2 where increase is mainly due to spin-orbit contribution.

Microscopic model for *E0* transition matrix elements

$$|a\rangle = |C_a,(1p_{1/2})^2\rangle \quad |b\rangle = |C_b,(0g_{9/2})^2\rangle$$ where C is ^{88}Sr core.

Example of ^{90}Zr, Experimental $\langle 0_1^+|r^2|0_2^+\rangle_{ch} = 1.70(3)\ fm^2$

Harmonic Oscillator (HO), core terms all cancel:

$$\langle 0_1^+|r^2|0_2^+\rangle = \frac{11}{2}b^2 - \frac{9}{2}b^2 = b^2$$

where $b^2 = \frac{\hbar}{m\omega}$. With $\hbar\omega = 45\mathrm{A}^{-1/3} - 25\mathrm{A}^{-2/3}$, $b^2 = 4.71\ \mathrm{fm}^2$

Consider finite charge and relativistic contributions: 5.32fm^2 where increase is mainly due to spin-orbit contribution.

E0 matrix element is closely connected to isomer shift between 1/2- GS and 9/2+ isomer.
Example of ^{89}Y, Experimental $\delta\langle r^2\rangle_{ch} = 0.84(8)\ fm^2$

$$\begin{aligned}\delta\langle r^2\rangle &= \langle C_b',0g_{9/2}|r^2|C_b',0g_{9/2}\rangle - \langle C_a',1p_{1/2}|r^2|C_a',1p_{1/2}\rangle \\ &= \langle C_b'|r^2|C_b'\rangle - \langle C_a'|r^2|C_a'\rangle \\ &\quad + \langle 0g_{9/2}|r^2|0g_{9/2}\rangle - \langle 1p_{1/2}|r^2|1p_{1/2}\rangle\end{aligned}$$

$\delta\langle r^2\rangle_{ch} = 5.31\ fm^2$

Microscopic model for *E0* transition matrix elements

Example of ^{90}Zr, Experimental $\langle 0_1^+ | r^2 | 0_2^+ \rangle_{ch} = 1.70(3)\ fm^2$

Replace wavefunctions with Skyrme self-consistent EDF:

Example of ^{89}Y, Experimental $\delta\langle r^2 \rangle_{ch} = 0.84(8)\ fm^2$

Microscopic model for *E0* transition matrix elements

Example of ^{90}Zr, Experimental $\langle 0_1^+ | r^2 | 0_2^+ \rangle_{ch} = 1.70(3)\ fm^2$

Replace wavefunctions with Skyrme self-consistent EDF:

Change in core radius

Spin-orbit

$$\langle 0_1^+ | r^2 | 0_2^+ \rangle = -4.00 + 4.10 + 0.61 = 0.71\ fm^2$$

Diff. in valence point proton radii

Example of ^{89}Y, Experimental $\delta \langle r^2 \rangle_{ch} = 0.84(8)\ fm^2$

Change in core radius

Spin-orbit

$$\delta \langle r^2 \rangle = -3.99 + 4.20 + 0.61 = 0.82\ fm^2$$

Diff. in valence point proton radii

Two-levels + inert core model

Microscopic model for *E0* transition matrix elements

Example of ^{90}Zr, Experimental $\langle 0_1^+ | r^2 | 0_2^+ \rangle_{ch} = 1.70(3)\ fm^2$

Replace wavefunctions with Skyrme self-consistent EDF:

Change in core radius

Spin-orbit

$$\langle 0_1^+ | r^2 | 0_2^+ \rangle = -4.00 + 4.10 + 0.61 = 0.71\ fm^2$$

Diff. in valence point proton radii

Example of ^{89}Y, Experimental $\delta\langle r^2 \rangle_{ch} = 0.84(8)\ fm^2$

Change in core radius

Spin-orbit

$$\delta\langle r^2 \rangle = -3.99 + 4.20 + 0.61 = 0.82\ fm^2$$

Diff. in valence point proton radii

Two-levels + inert core model, next replace with CI occupations

Microscopic model for *E0* transition matrix elements

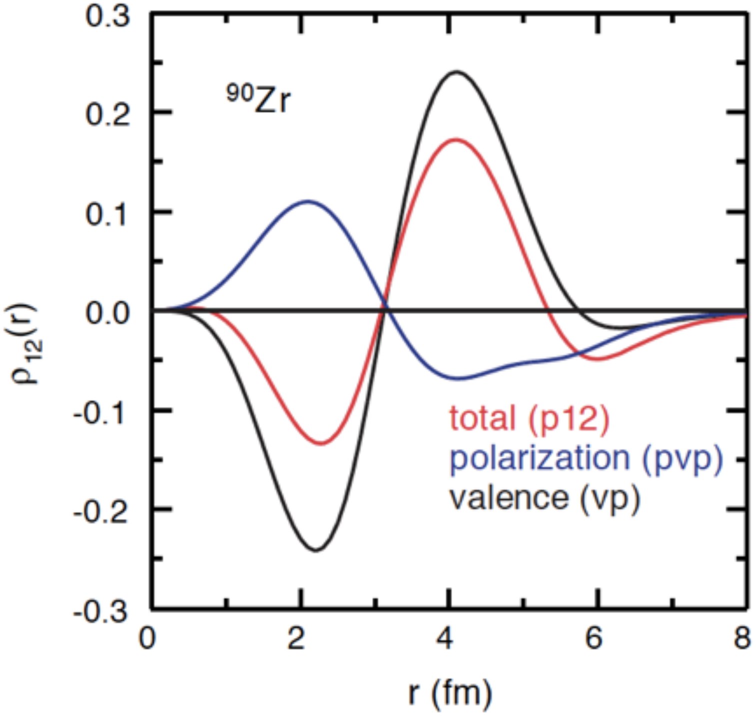

Proton radial transition density from difference of initial and final states.

Large orbital-dependent effect of core polarization from the valence nucleons.

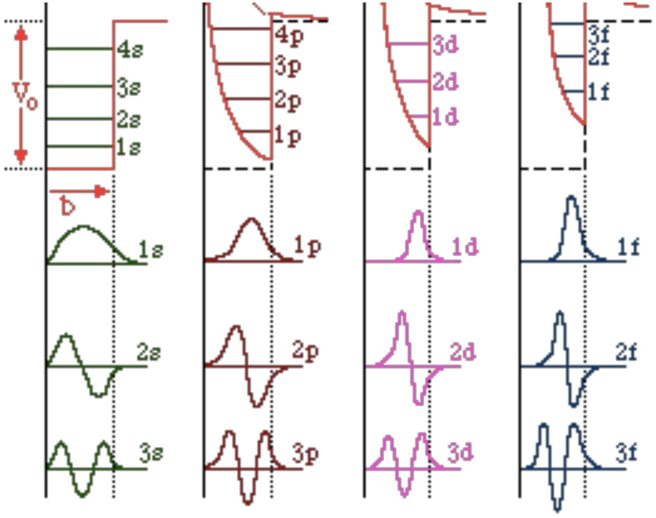

Radial wavefunctions $\mathbf{R}_{nl}$

Microscopic model for *E0* transition matrix elements

Form factors from inelastic electron scattering on ^{26}Mg

H. Blok *et al.*, PLB 149, 441 (1984).

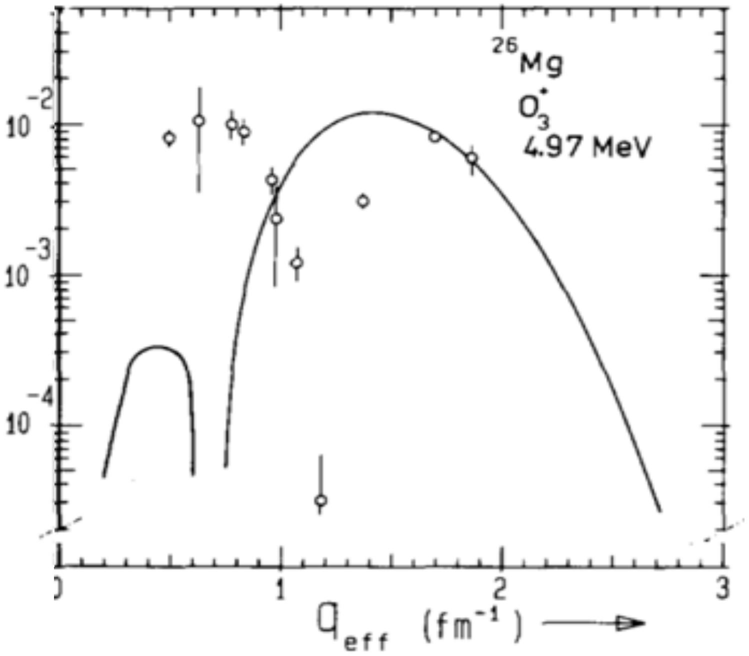

Better agreement from adding an arbitrary small amount of $0d_{5/2}$-$1d_{5/2}$ and $0f_{7/2}$-$1f_{7/2}$ to off-diagonal transition density.

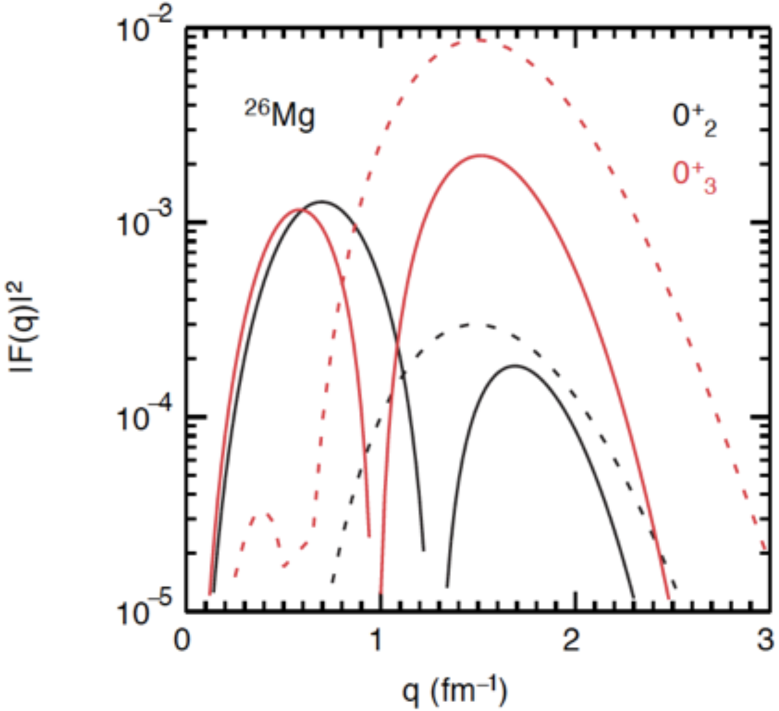

Core polarization model equivalent to addition of giant monopole transition density

Microscopic model for *E0* transition matrix elements

Agreement is very good for large range of *A* and different active particles.

Result is sensitive to Skyme parameters and may provide new constraints for them.

$$\rho(E0) = \frac{\langle f | M(E0) | i \rangle}{eR^2}$$

E0 Nuclear matrix element

		0^+-0^+ i-f	Exp.	New Model s3	New Model skx	Spin orbit
Valence protons	^{90}Zr	2-1	1.70(3)	0.57	0.90	0.53
Valence neutrons	^{206}Pb	2-1	1.72(6)	1.43	0.66	-0.04
	^{68}Ni	2-1	1.41(3)	0.74	1.06	0.43
Valence protons and neutrons	^{58}Ni	2-1	0.054(14)	1.80	1.47	0.33
	^{58}Ni	3-1	5.5(10)	2.62	1.69	-0.08
	^{32}S	3-1	2.0(3)	1.06	0.74	-0.04
	^{26}Mg	2-1	3.5(12)	1.11	0.93	0.16
	^{26}Mg	3-1	3.8(10)	1.79	1.40	0.00

B.A. Brown *et al.*, PRC 95, 011301(R) (2017).
Skyme parameter sets from B.A. Brown *et al.*, PRC 92, 014305 (2015).

Microscopic model for *E0* transition matrix elements

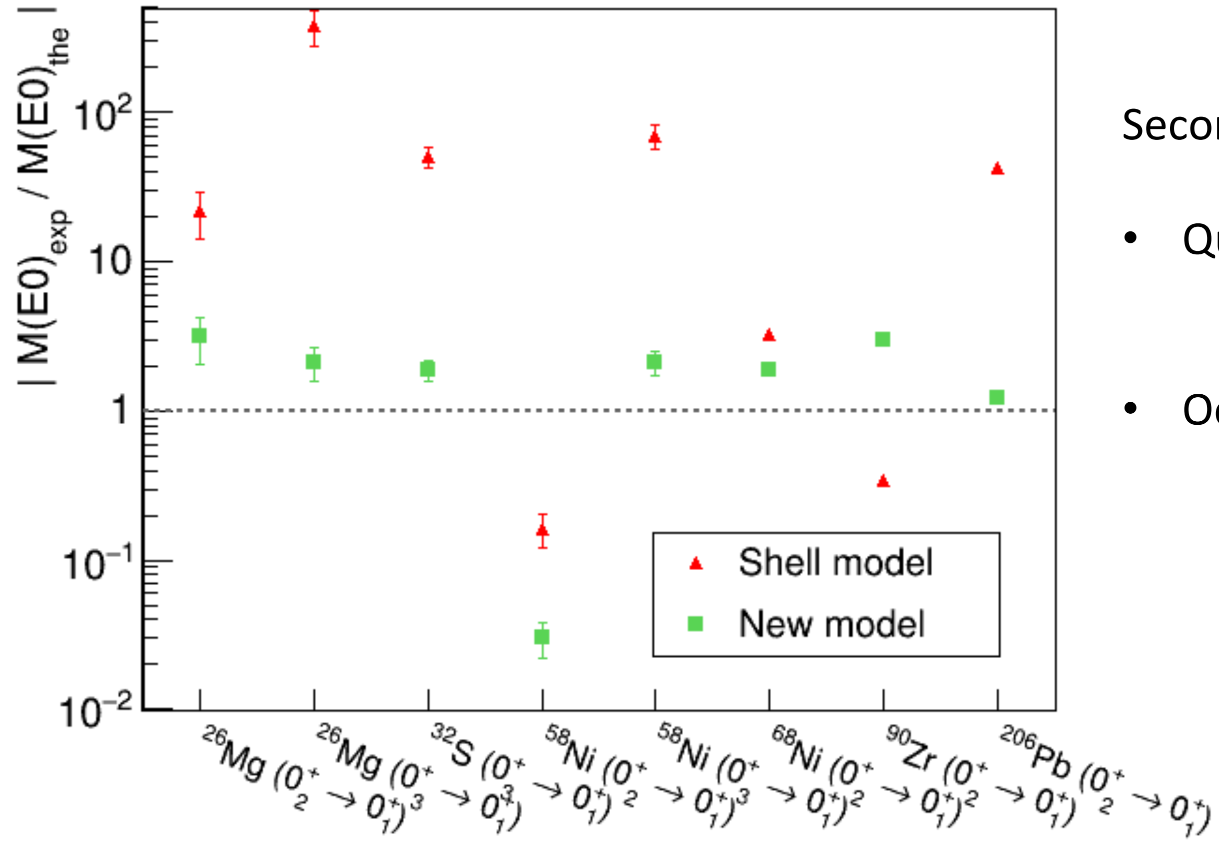

Second-order corrections:

- Quadrupole zero-point motion
  eg. $[2^+_v \otimes 2^+_{coll}]^{j=0+}$ admixtures
- Octupole correlations

B.A. Brown *et al.*, PRC 95, 011301(R) (2017).
Skyme parameter sets from B.A. Brown *et al.*, PRC 92, 014305 (2015).

Outline

- A microscopic model for *E0* transition matrix elements
- First measurement of 2-2 *E0* strengths in spherical nuclei – ^{58,60,62}Ni at ANU
- Shape coexistence studies at TRIUMF-ISAC using gamma-ray and electron spectroscopy
- Questions and observations

PhD Thesis of Lee Evitts
(TRIUMF/Univ. of Surrey)

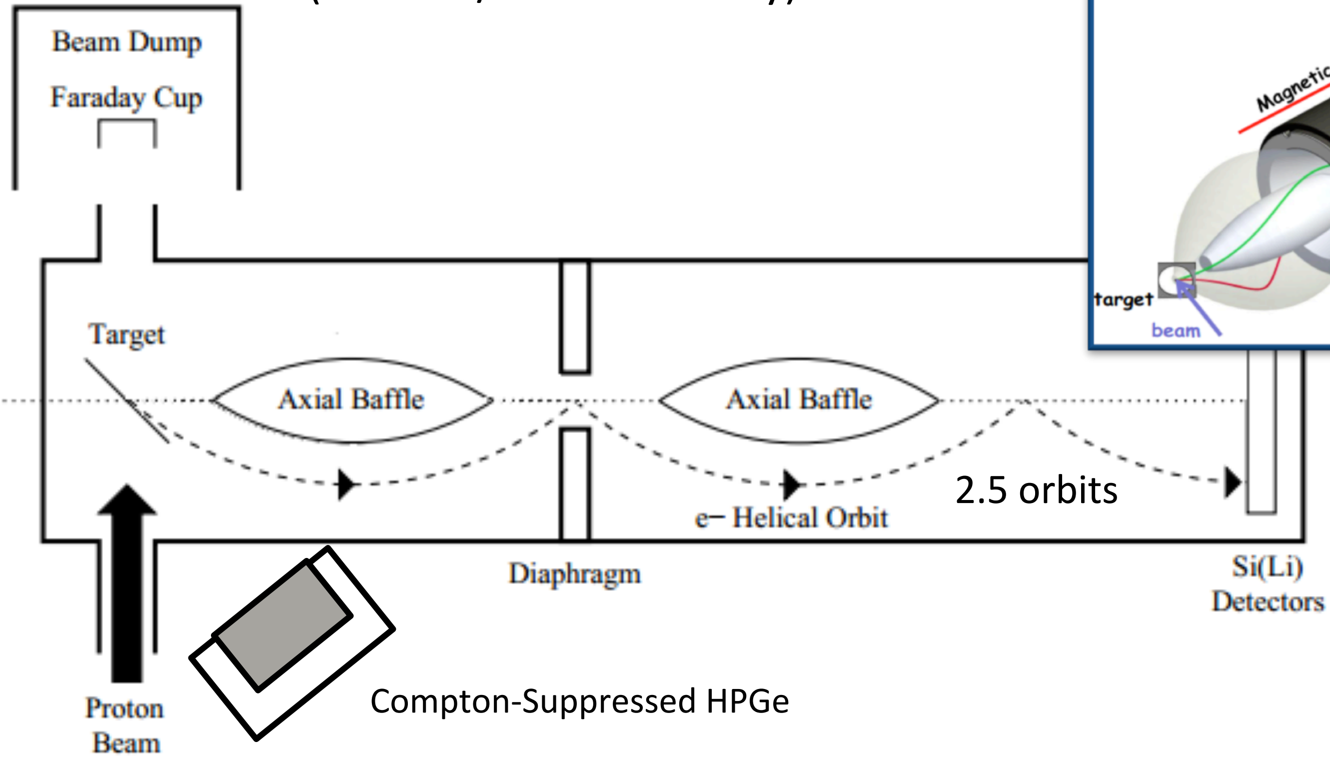

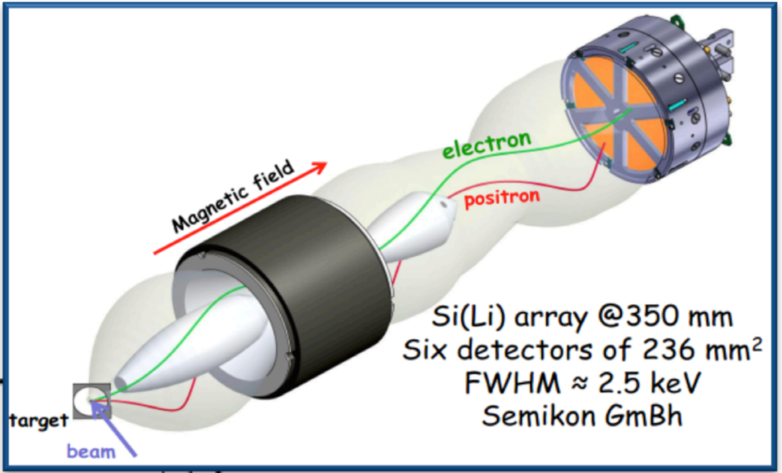

Inelastic proton scattering on ^{58,60,62}Ni targets
1.4-1.6mg/cm^2
<9.2MeV protons

Super-e at ANU

Magnetic field operated in a sweeping mode with fixed beam integration at each step.

SWEEPING

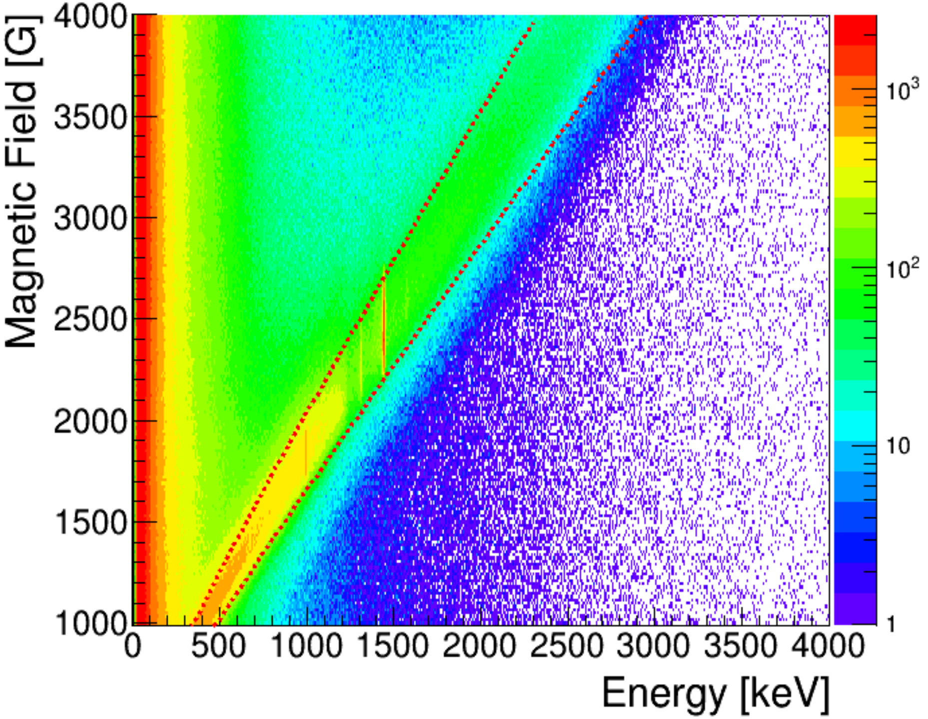

Momentum gate improves peak-to-background of e- spectrum

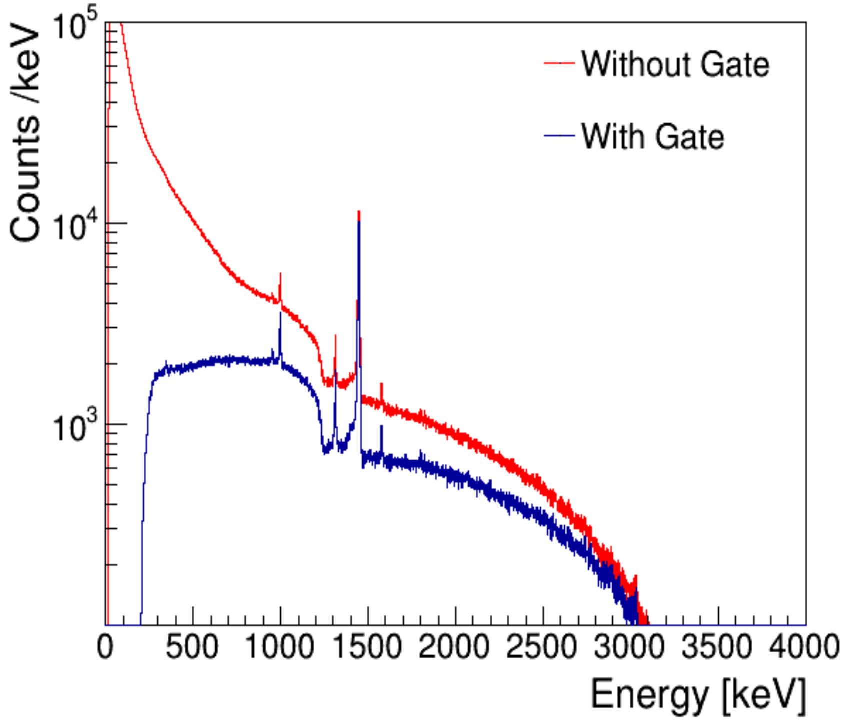

^{170}Lu as calibration source

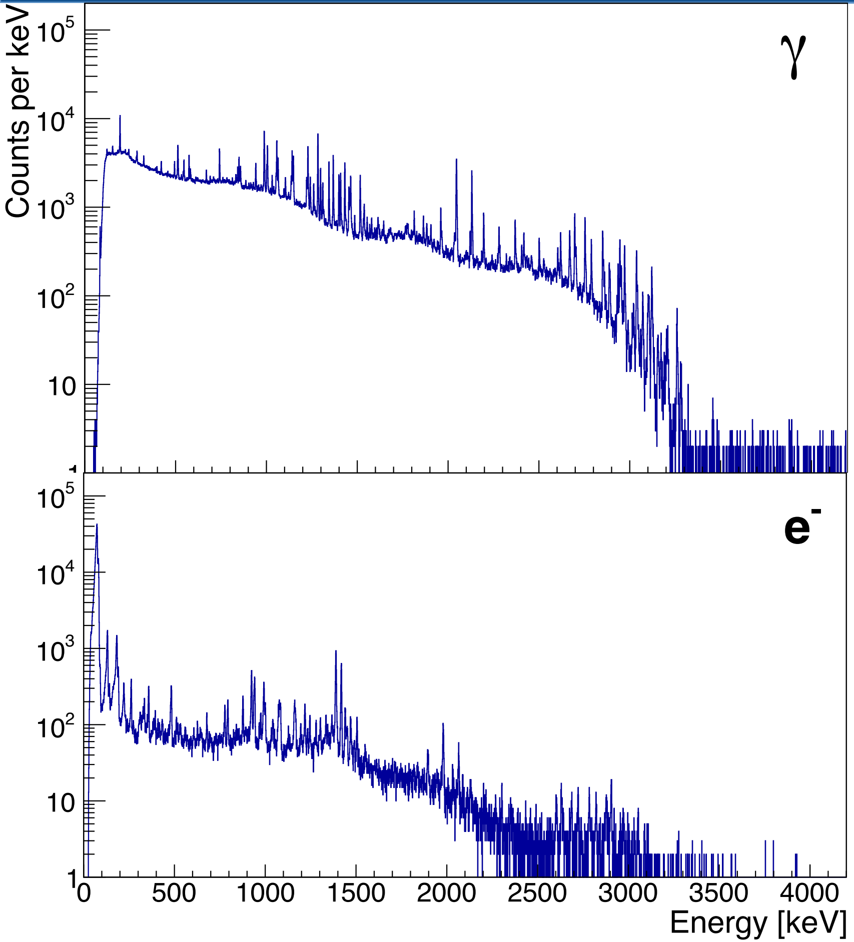

^{170}Lu to ^{170}Yb Electron Capture.
Q value = 3459 (19) keV.
Half-life is 2.012(21) days.

Relative intensities and ICC known to good precision from several studies.

Produced by ^{171}Yb(p,2n) at 18MeV.
Alternatively produced by ISOL.

^{170}Lu source ($T_{1/2}$=2 days) produced by ^{171}Yb(p,2n)

Gamma relative efficiency

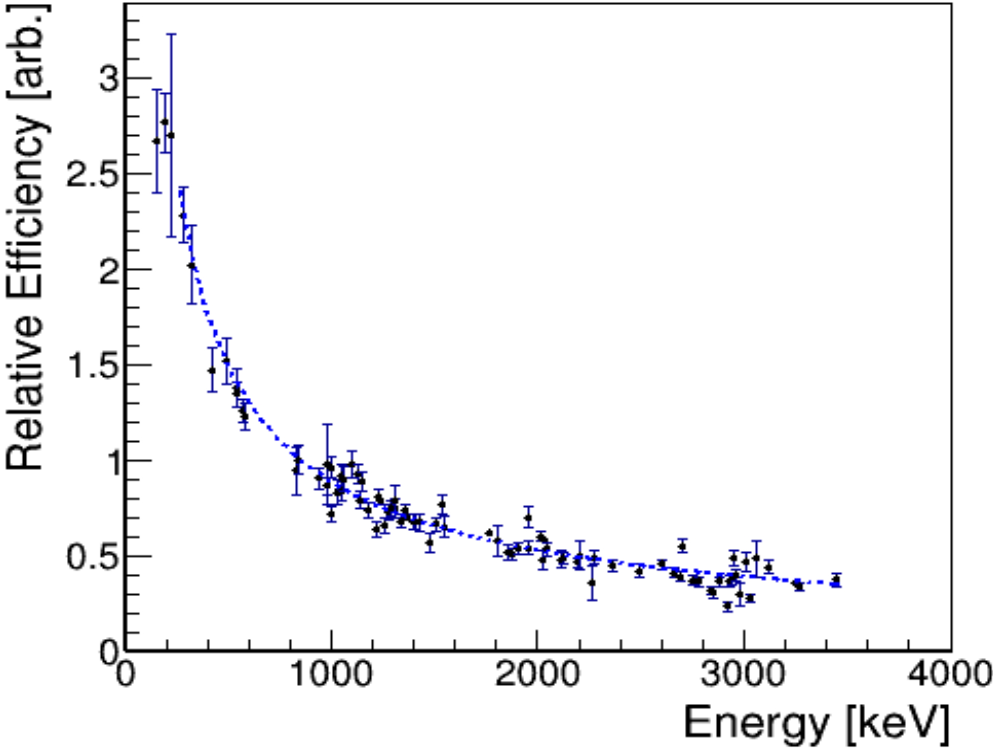

Electron relative efficiency

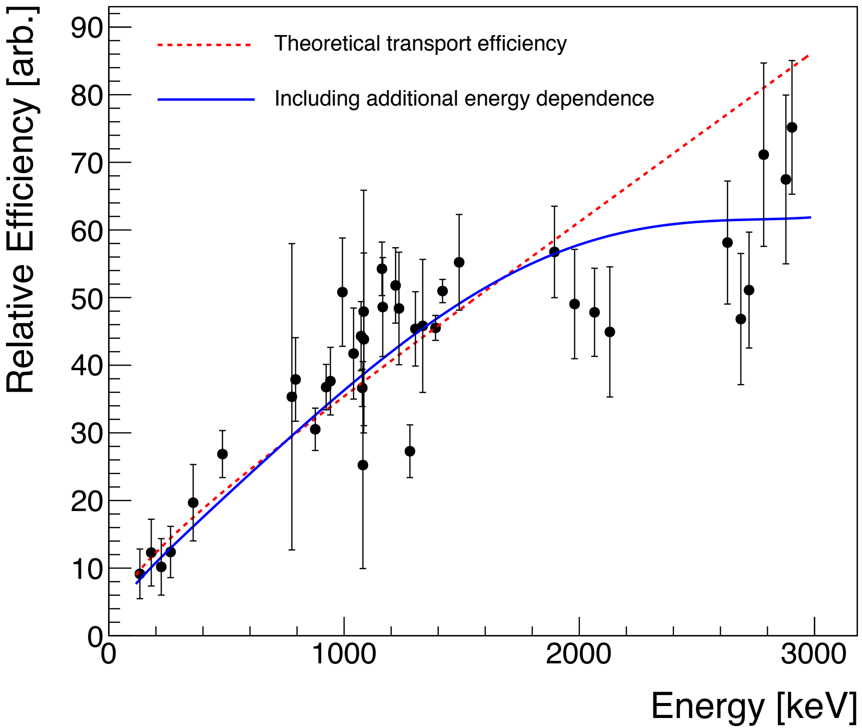

(E2/M1) mixing ratio measurements

Gamma-ray angular distributions using the CAESAR array to determine δ(E2/M1) mixing ratios.

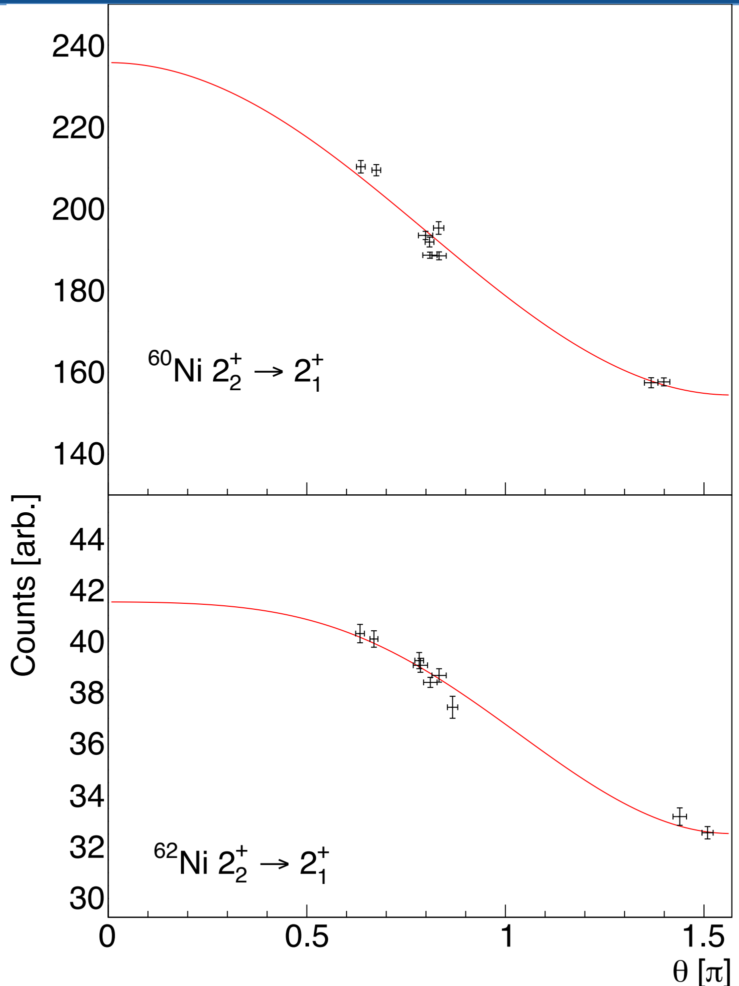

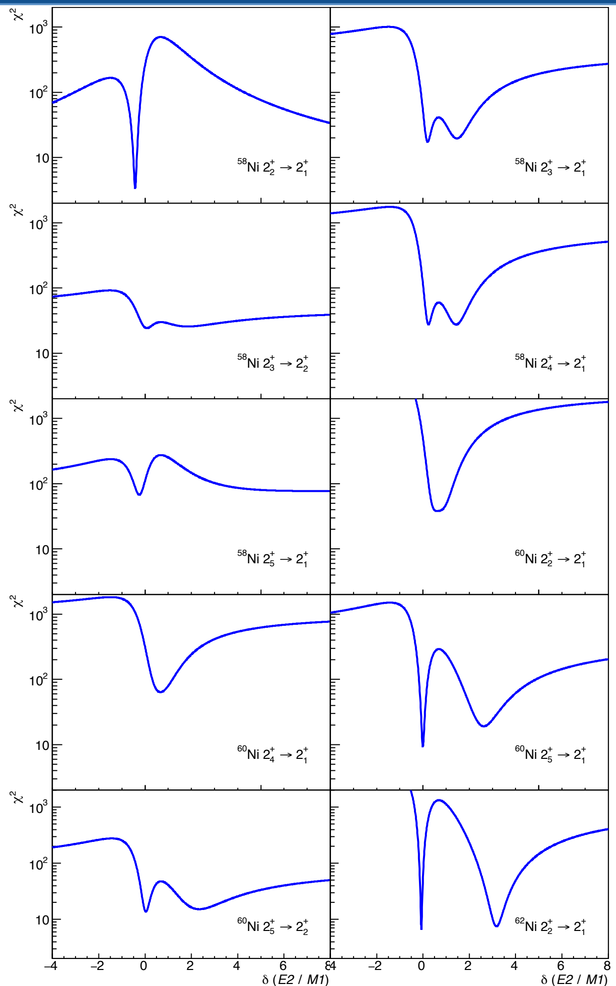

Internal conversion electron measurements

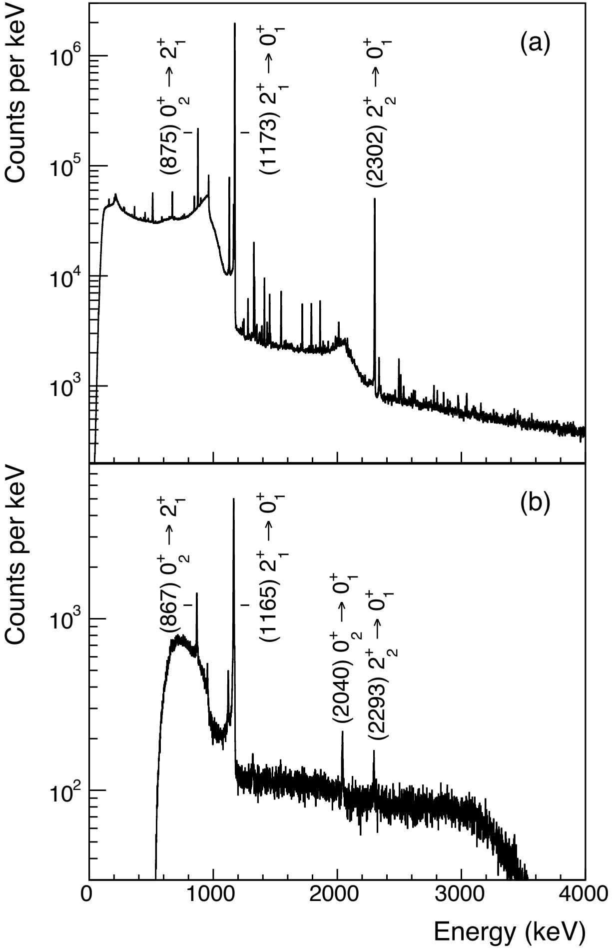

- Multiple peaks fitted simultaneously
- K-L energy difference fixed
- For Pure E2: intensity ratio of K and L fixed
- Higher than L omitted (<1.5%)
- Reduced chi-squared below = 1.2

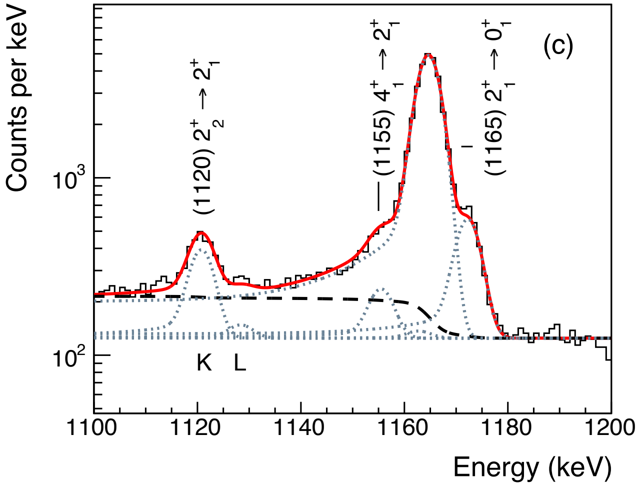

$$\alpha = \frac{\lambda_{IC}}{\lambda_{\gamma}}$$

ICC measured

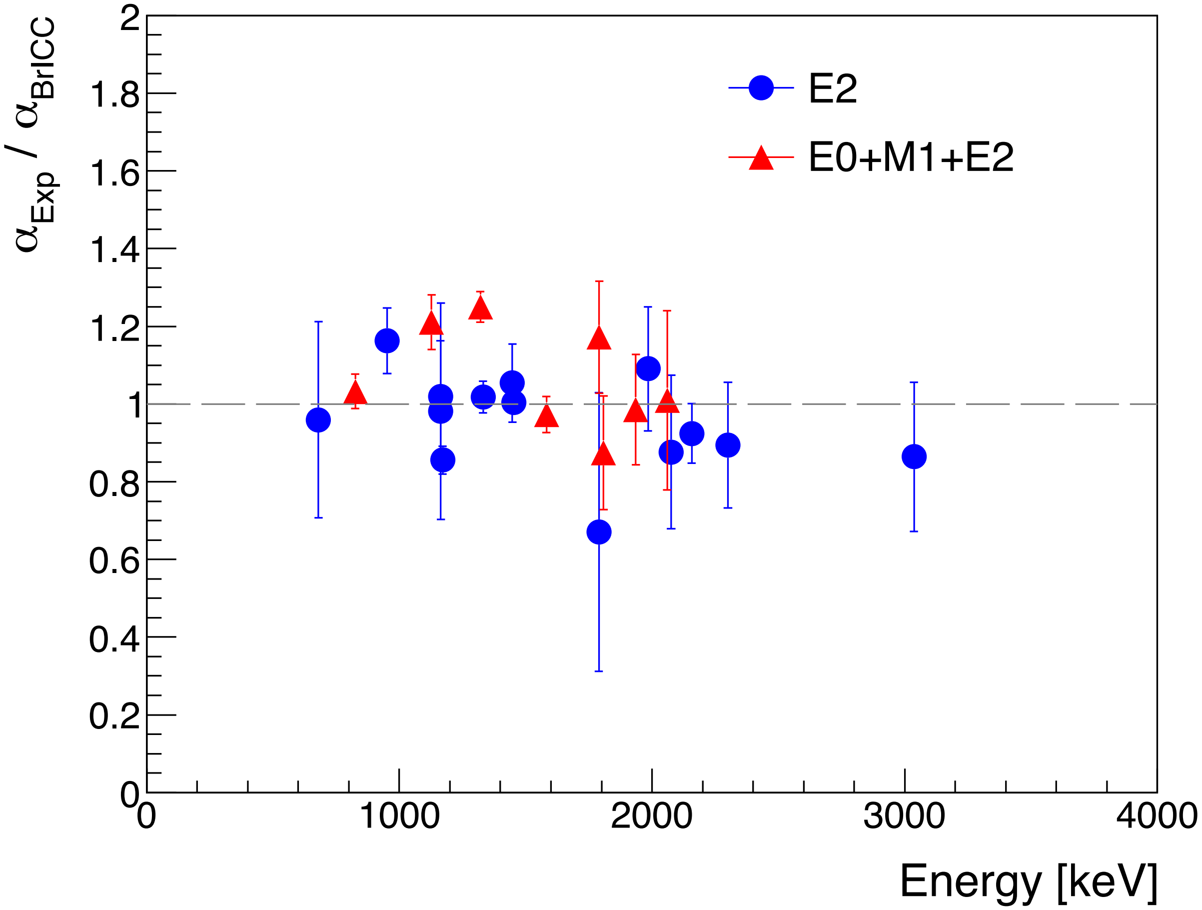

Pure E2 ICC are well reproduced.

Some mixed transitions indicate significant E0 components.

Handling of asymmetric uncertainties

Monte Carlo method used for value and error determination.

- Treat all input values as a normal probability distribution (μ,σ).
- Output is not a normal distribution.
- Uncertainty obtained from region containing 68% with $y(x_1)=y(x_2)$.

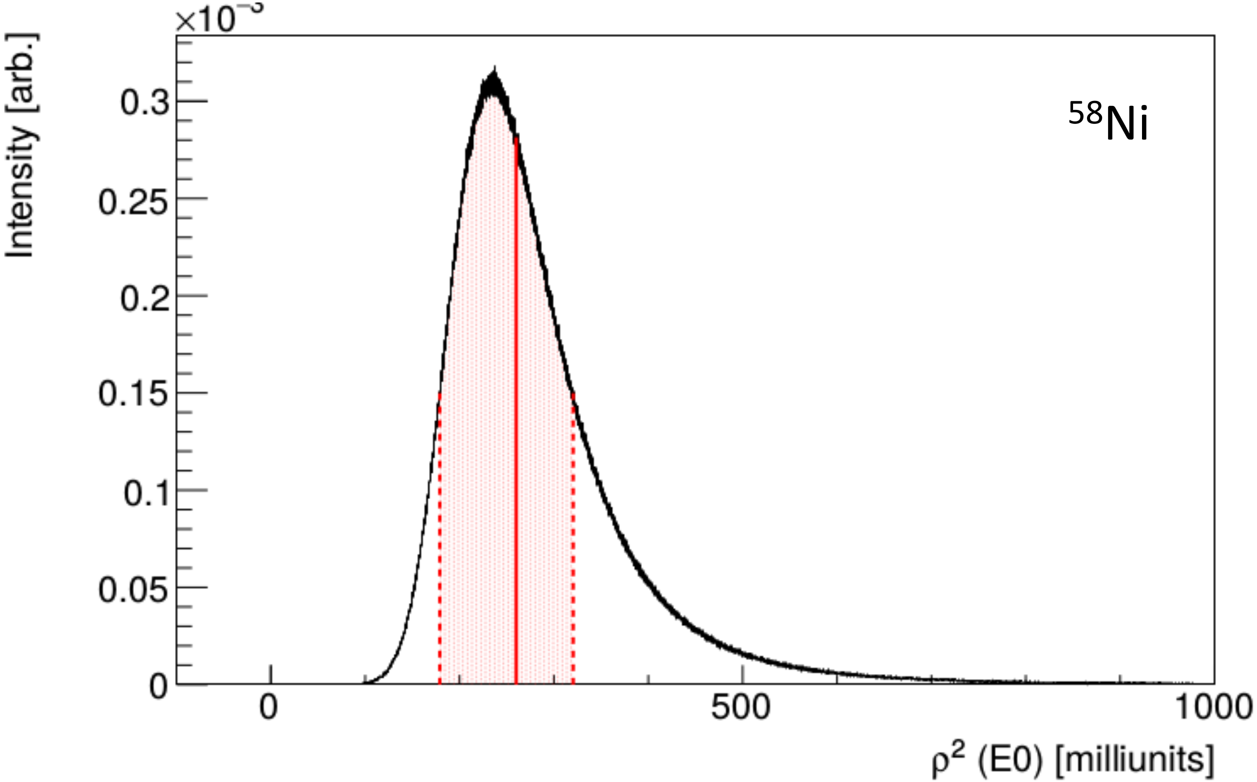

Identification of significant E0 strength in the 2_2-2_1 transitions of ^{58,60,62}Ni

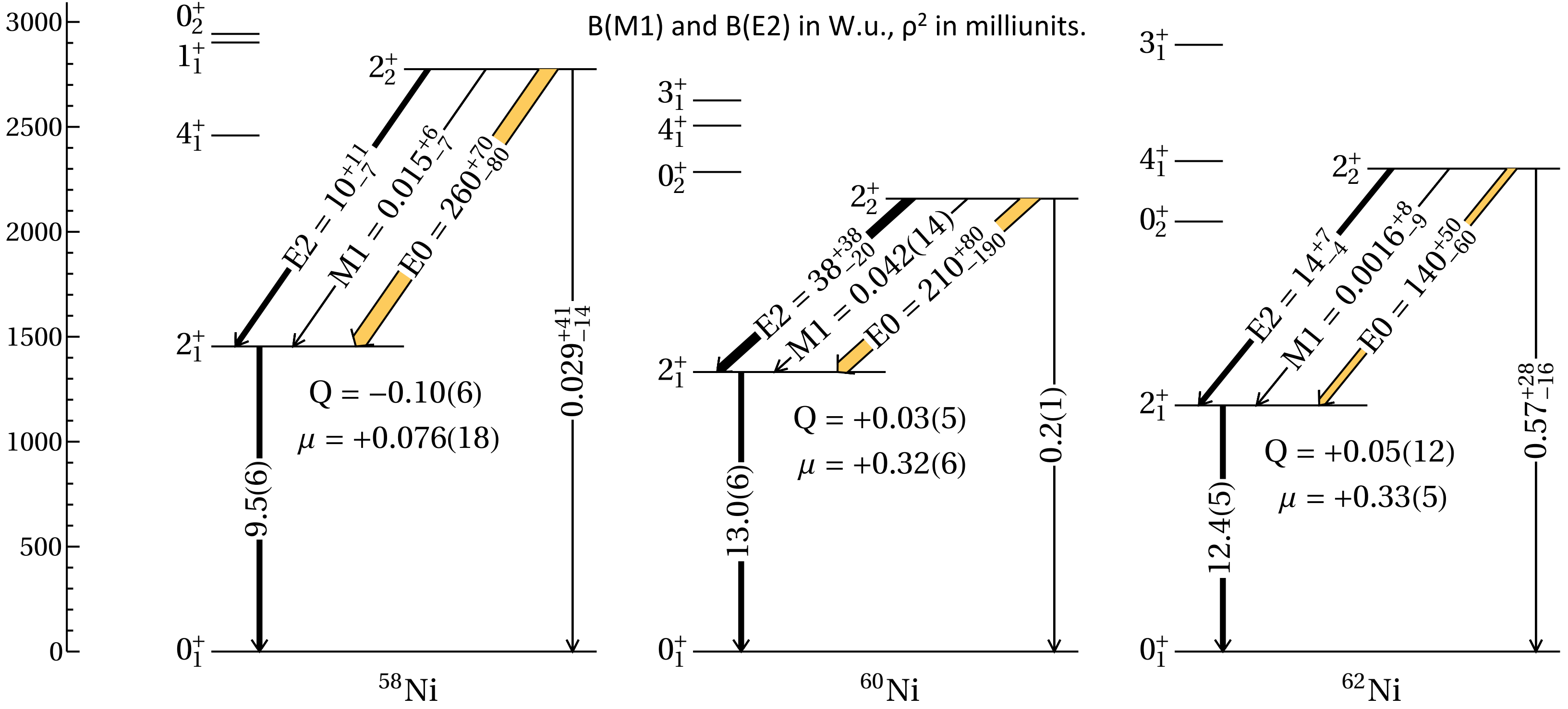

	E_γ (keV)	$T_{1/2}$ (ps)	I_γ	$\delta(E2/M1)$	$\alpha_K \times 10^4$	B($M1$)	B($E2$)	$M(E0)$	$\rho^2(E0).10^3$
^{58}Ni	1321.2	$0.38^{+0.12}_{-0.09}$	96(3)	-0.78(32)	1.4(3)	$0.015^{+0.006}_{-0.007}$	10^{+11}_{-7}	$11.0^{+1.4}_{-1.9}$	260^{+70}_{-80}
^{60}Ni	826.06	0.59(17)	85(2)	+0.58(14)	3.0(1)	0.042(14)	38^{+38}_{-20}	10^{+2}_{-7}	210^{+80}_{-190}
^{62}Ni	1128.82	$0.58^{+0.16}_{-0.09}$	45(2)	+2.5(6)	2.0(1)	$0.0016^{+0.0008}_{-0.0009}$	14^{+7}_{-4}	$8.4^{+1.4}_{-2.1}$	140^{+50}_{-60}

Identification of significant E0 strength in the 2_2-2_1 transitions of ^{58,60,62}Ni

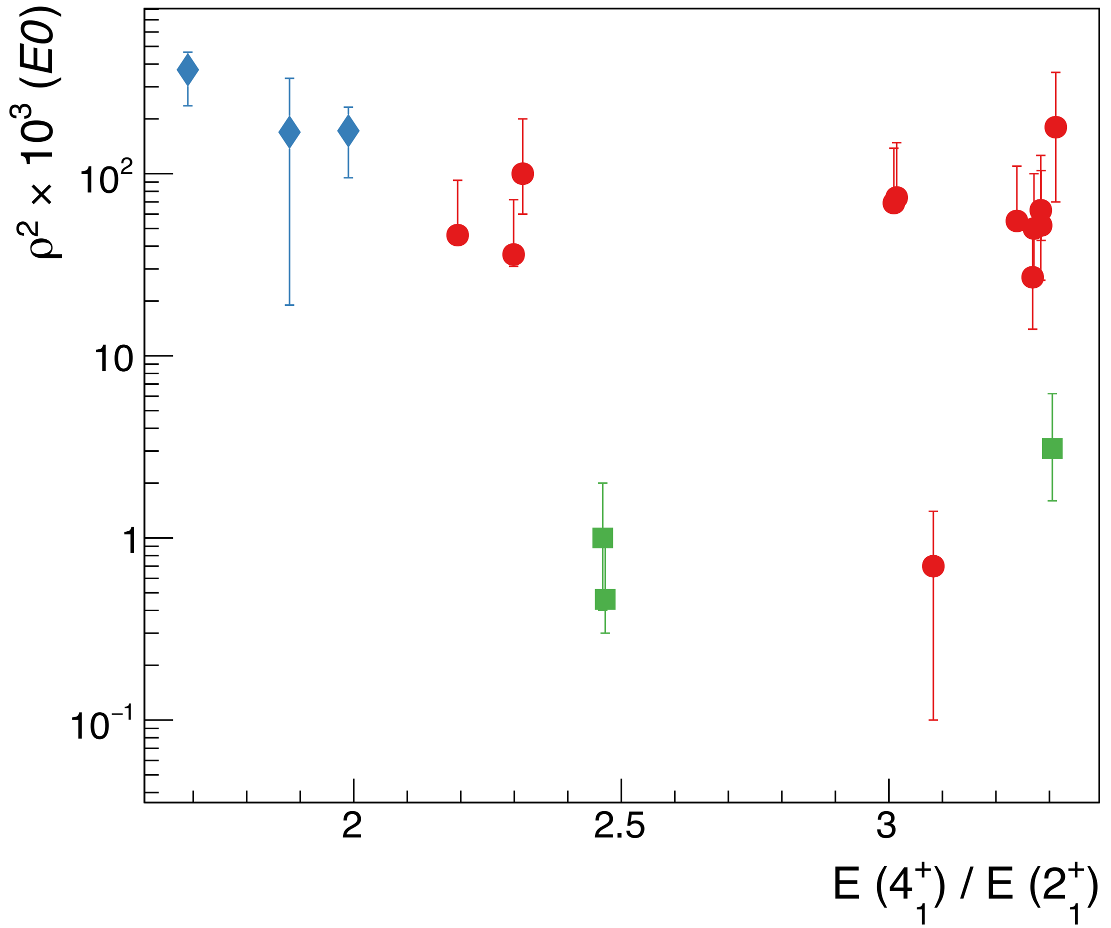

(diamond) Ni isotopes.

Literature values grouped by the sign of Q_s $(2_1{}^+)$:
(circles) prolate,
(square) oblate.

Data from compilation by Wood et al., NPA 651, 323 (1999).

Microscopic model for *E0* transitions

Good reproduction for 0-0 but not for 2-2 transitions.

Table 3: Calculated and experimental properties of the first and second 2^+ states in ^{58,60,62}Ni.

Theory	B($M1$) $2_2^+ \to 2_1^+$ μ_N^2	B($E2$) $2_2^+ \to 2_1^+$ $e^2 fm^4$	μ 2_1^+ μ_N	Q 2_1^+ efm^2	$M(E0)$ Skx $(s3)$ fm^2	E_2 2_2^+ MeV	E_1 2_1^+ MeV
^{58}Ni	0.165	30.3	-0.14	-2.7	1.66(0.80)	2.64	1.48
^{60}Ni	0.044	269	0.30	2.3	0.38(0.50)	2.29	1.56
^{62}Ni	0.0039	151	0.61	25.3	0.53(1.06)	2.34	1.15

Experiment	B($M1$) $2_2^+ \to 2_1^+$ μ_N^2	B($E2$) $2_2^+ \to 2_1^+$ $e^2 fm^4$	μ 2_1^+ μ_N	Q 2_1^+ efm^2	$M(E0)$ fm^2	E_2 2_2^+ MeV	E_1 2_1^+ MeV
^{58}Ni	0.027^{+11}_{-13}	133^{+147}_{-93}	0.076(18)	-10(6)	$11.0^{+1.4}_{-1.9}$	2.77	1.45
^{60}Ni	0.075^{+25}_{-25}	530^{+530}_{-279}	0.32(6)	3(5)	10^{+2}_{-7}	2.16	1.33
^{62}Ni	0.0028^{+14}_{-16}	204^{+102}_{-58}	0.33(5)	5(12)	$8.4^{+1.4}_{-2.1}$	2.30	1.17

Second-order corrections may be needed – coupling valence nucleons to the 1p-1h giant quadrupole excitation.

Outline

- A microscopic model for *E0* transition matrix elements
- First measurement of 2-2 *E0* strengths in spherical nuclei – ^{58,60,62}Ni at ANU
- Shape coexistence studies at TRIUMF-ISAC using gamma-ray and electron spectroscopy
- Questions and observations

TRIUMF-ISAC

Isotope Separator and ACcelerator

1 RIB delivery to experiments

500MeV p^+ at 100μA on ISOL target

SiC, NiO, Nb, ZrC, Ta, UC_x Targets
Surface, FEBIAD, IG-LIS ion sources

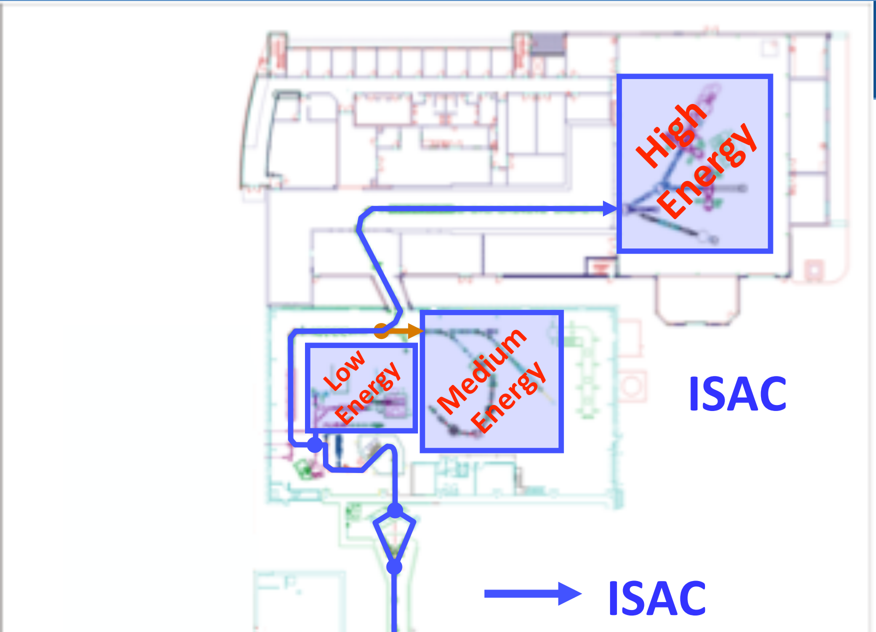

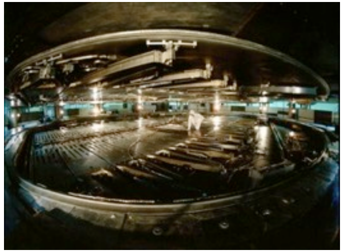

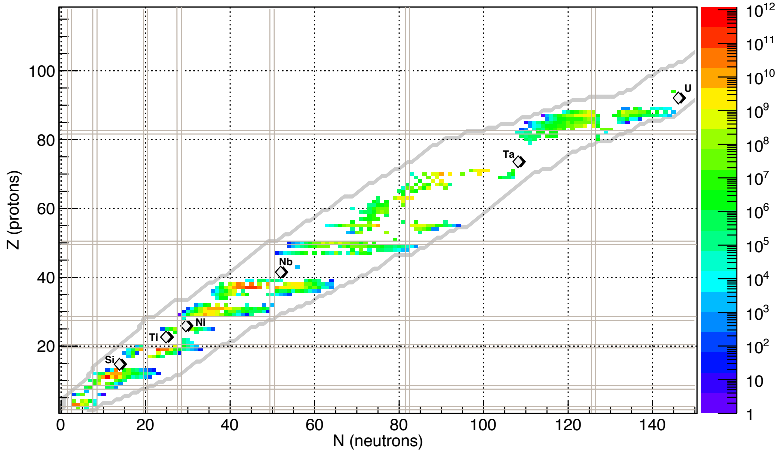

ISAC-I Low-Energy	<60keV	Ground state + decay, material science
ISAC-I Medium E	<1.5MeV/u	Astrophysics
ISAC-II SC LINAC	<10MeV/u	Nuclear reactions and structure

TRIUMF-ARIEL

Advanced Rare-IsotopE Laboratory

1 RIB ➔ 3 simultaneous RIBs

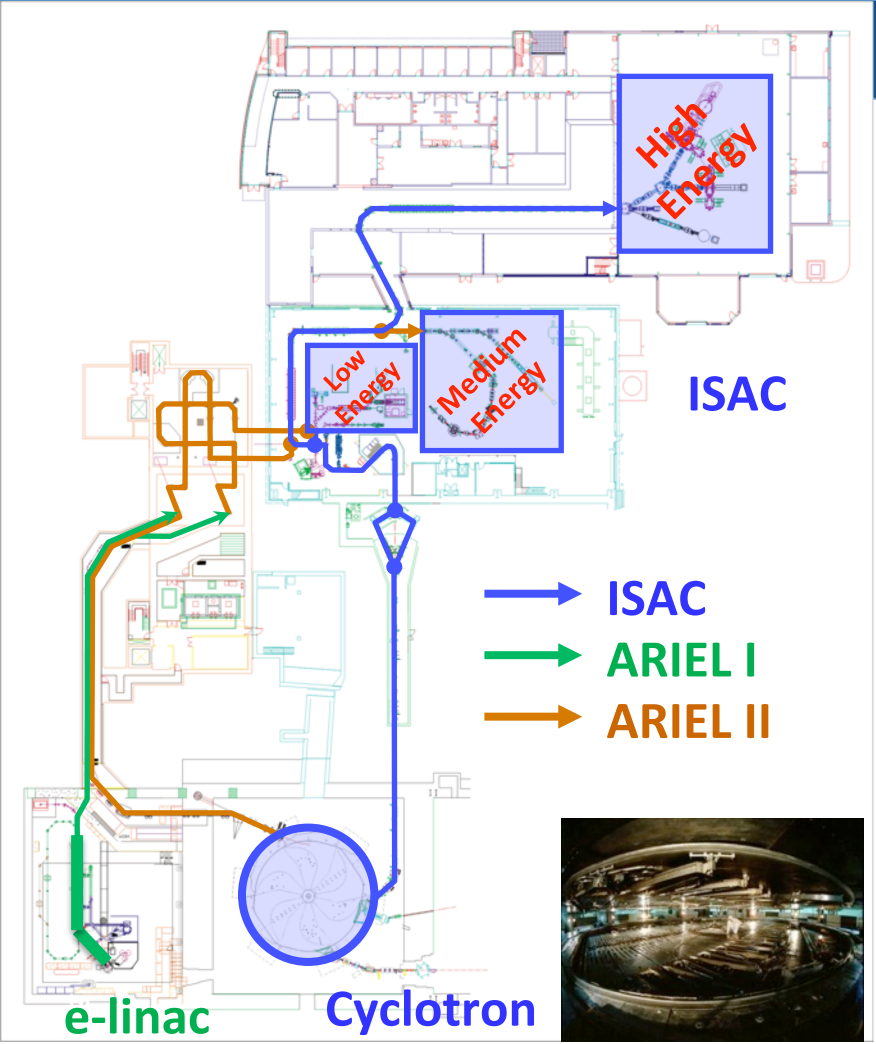

ARIEL Project:

- new electron linac driver for photo-fission
- new target stations and front end
- new proton beamline

E-linac and electron beamline
Sept. 2014

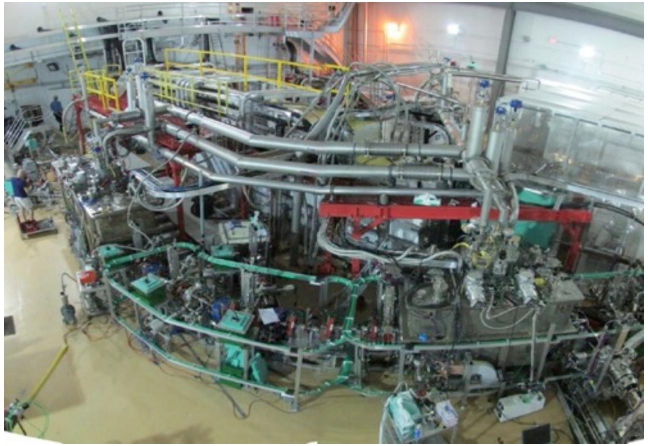

ARIEL beams to ISAC experiments

Rare-isotope beams will be produced by from proton and electron driver beams.

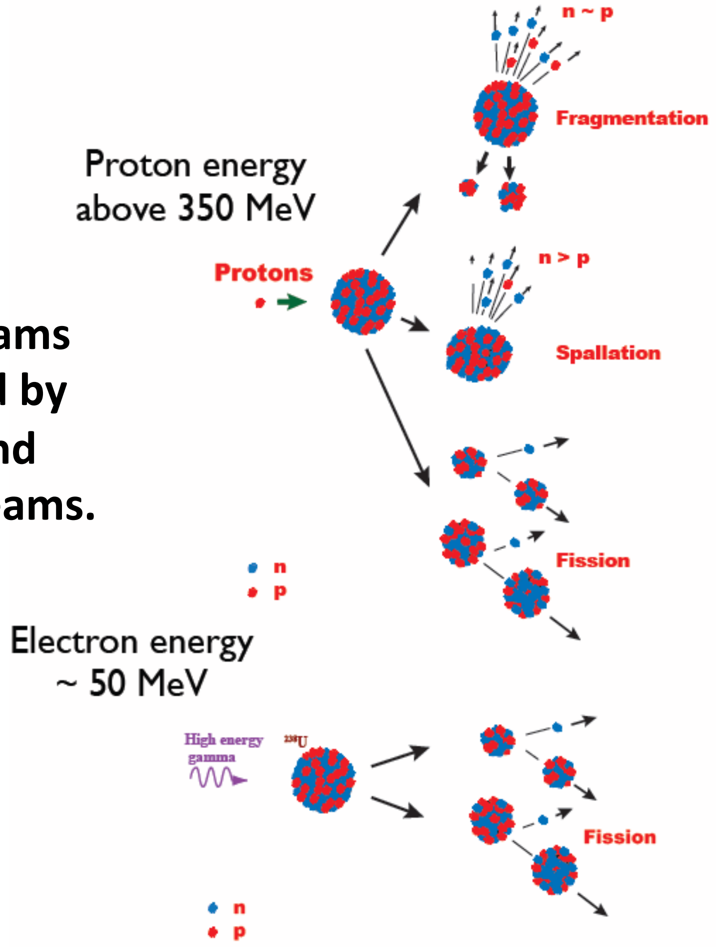

500MeV Protons on UCx

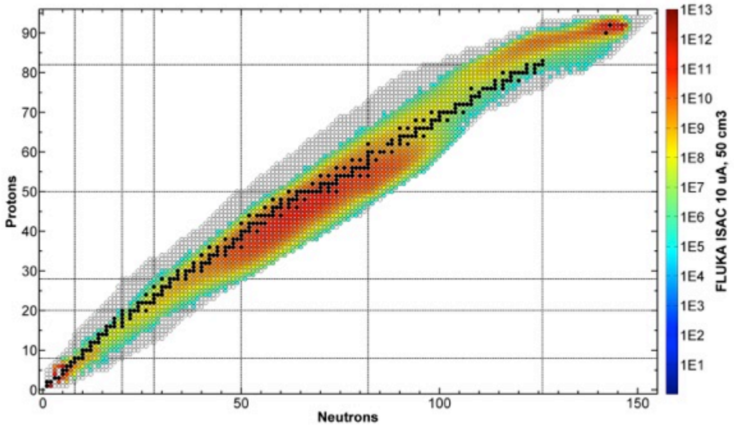

Photo-fission of UCx

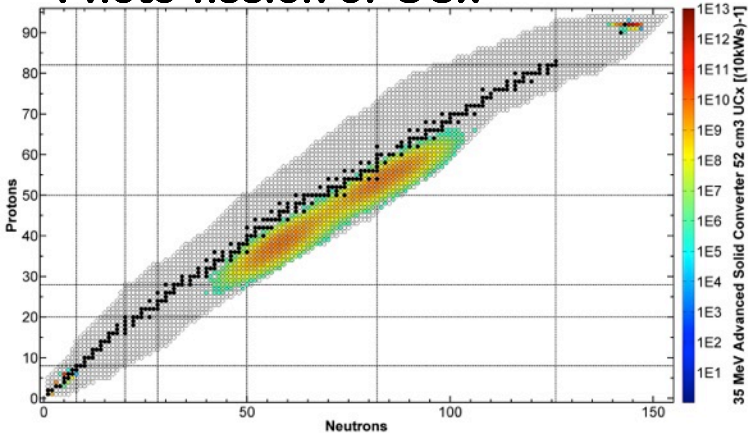

TRIUMF

ARIEL Completion to Science

1999	Low-energy ISAC beams
10/2019	ISAC-CANREB-ISAC beams
03/2022	ARIEL beam to β-NMR
06/2022	ARIEL photo-fission beams to ISAC
03/2023	ARIEL spallation beams to ISAC

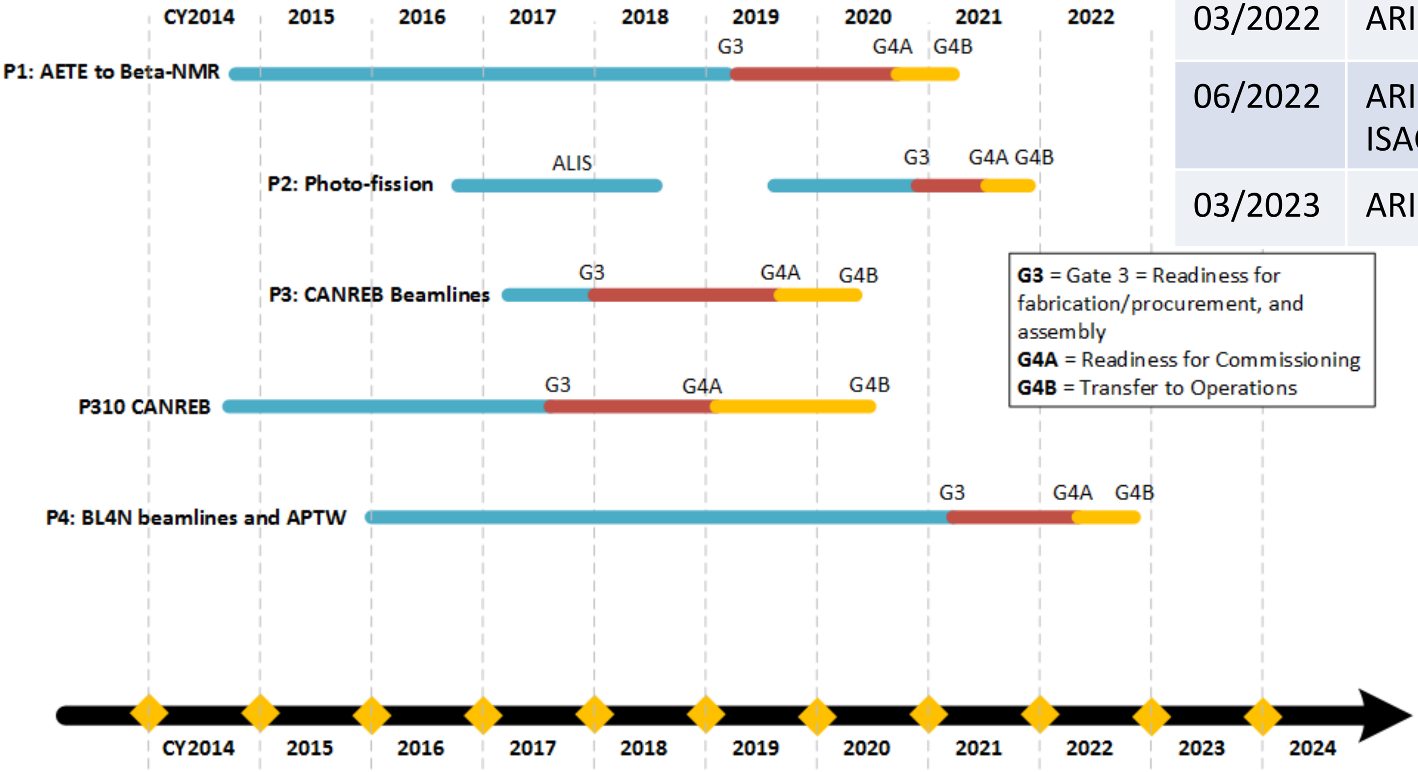

Gamma-Ray and Electron Spectroscopy at ISAC

GRIFFIN
Precision studies with stopped RIBs

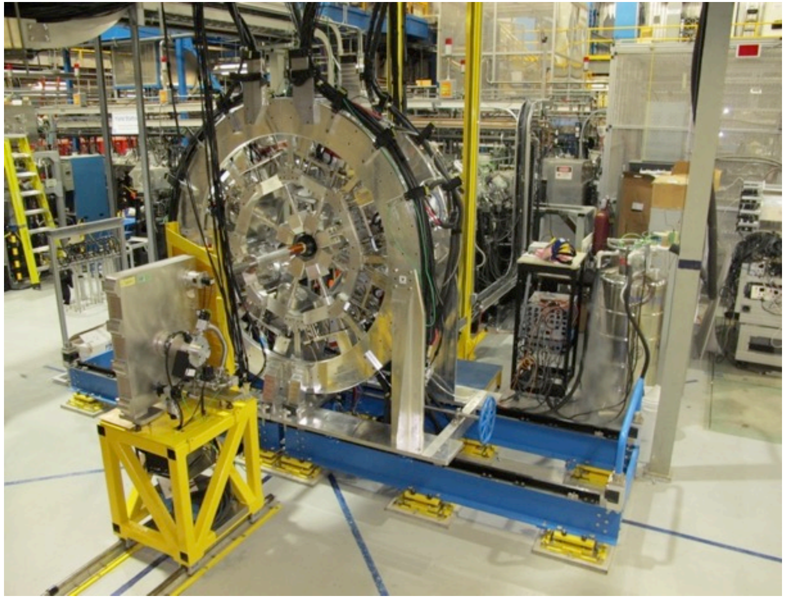

TIGRESS
Experiments with accelerated RIBs

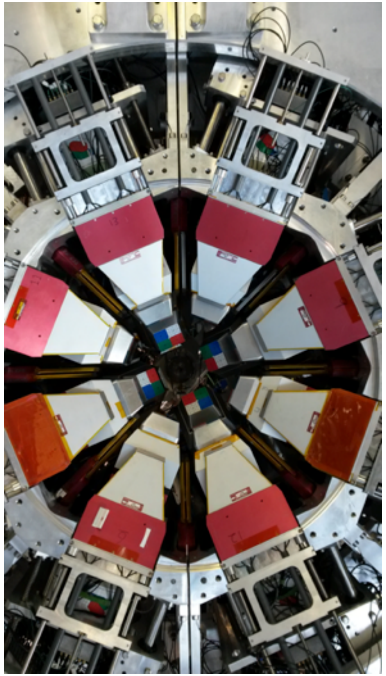

Decay spectroscopy

GRIFFIN
Precision studies with stopped RIBs

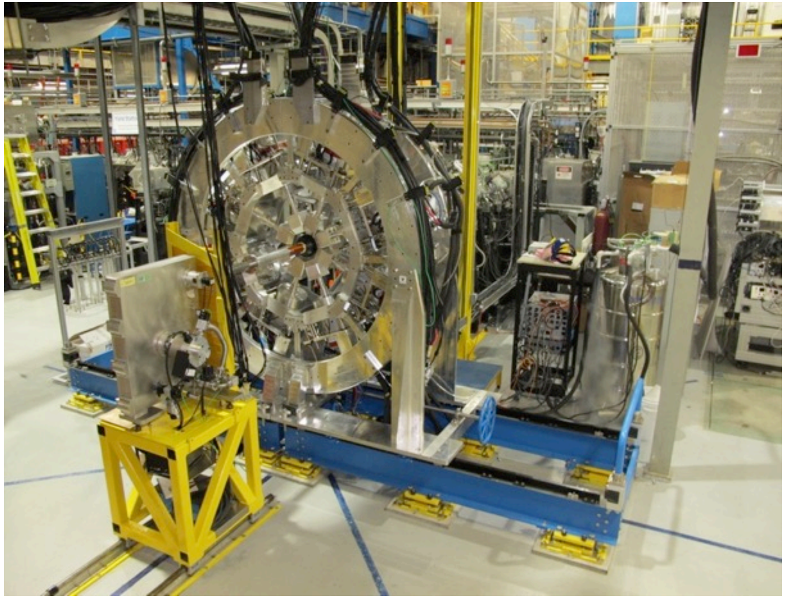

PACES – electron spectrometer

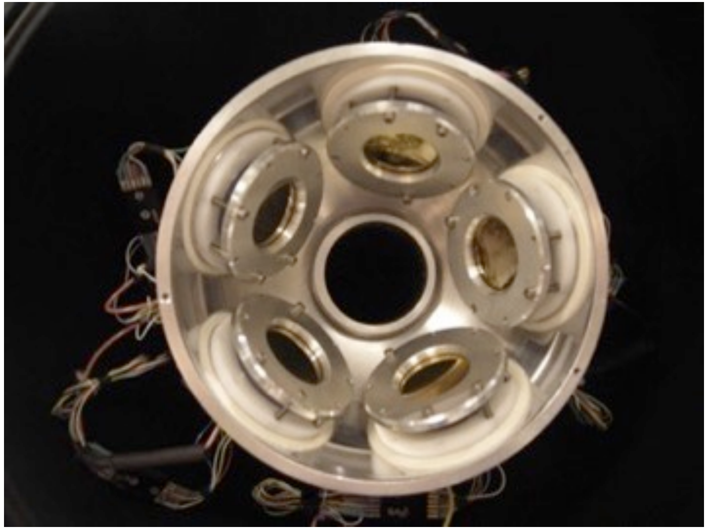

In-beam spectroscopy with accelerated RIBs

SPICE – in-beam electron spectrometer

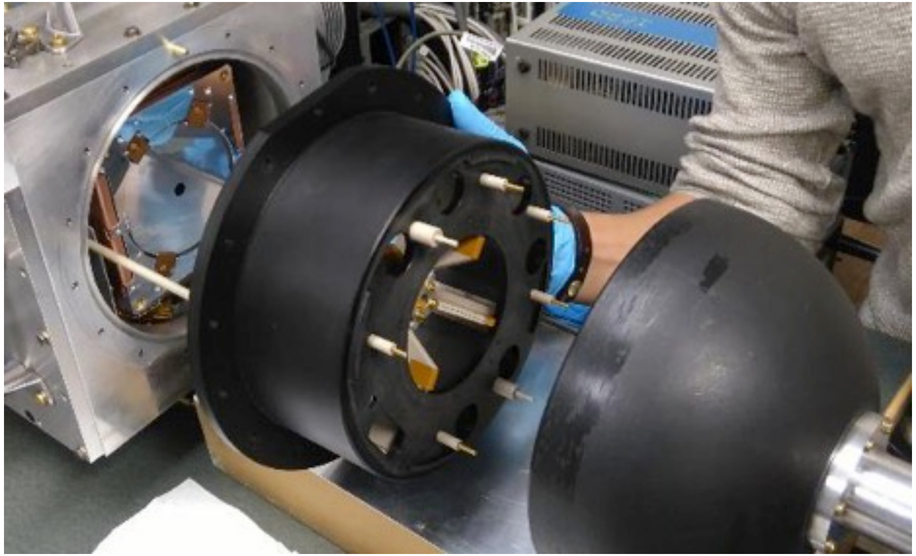

TIGRESS
Experiments with accelerated RIBs

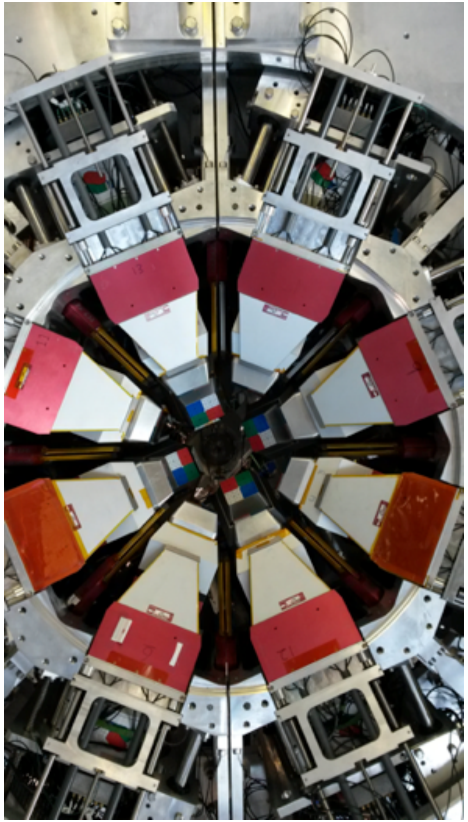

ISAC-II High Mass: ^{156,158,160}Er Coulomb Excitation with TIGRESS

A>29 beams require charge-breeding.
- Currently use ISAC CSB
- CANREB EBIS from 2019

S1750, J. Smallcombe & A.B. Garnsworthy
HPTa target with TRILIS and CSB.
Beams delivered to TIGRESS, Oct 2017:

$^{156}Er^{23+}$: 1×10^8 total pps, 25% ^{156}Er, ~14hrs
$^{158}Er^{23+}$: 1×10^8 total pps, 50% ^{158}Er, ~14hrs
$^{160}Er^{23+}$: 1×10^8 total pps, 50% ^{160}Er, ~14hrs

3.9MeVA Coulex on ^{58}Ni target

Will measure quadrupole moments of low-lying states to determine the shape of these nuclei, and investigate coexistence at *N*=88,90.

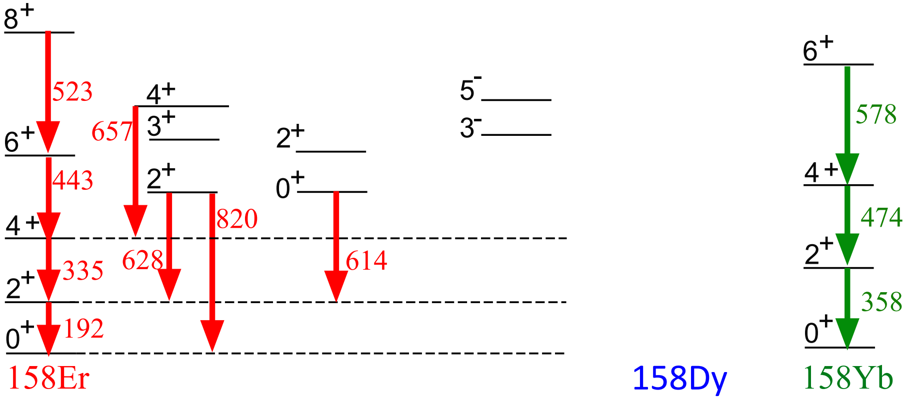

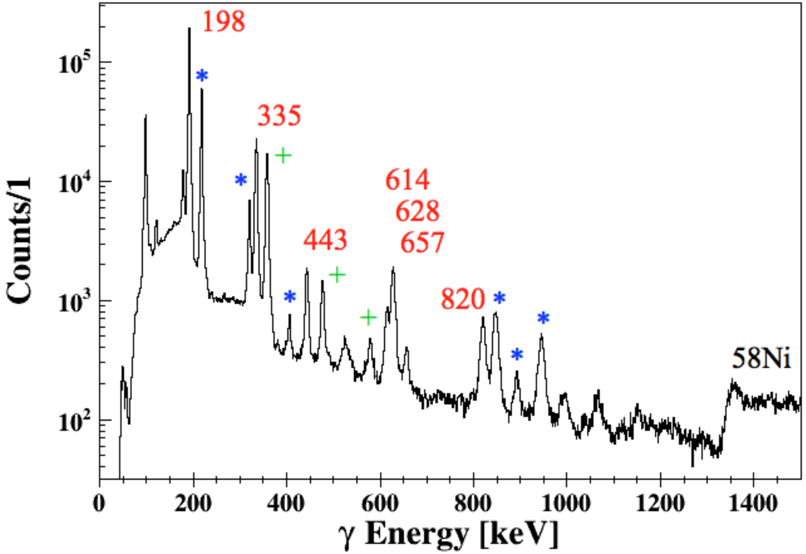

The GRIFFIN Spectrometer for precision decay studies

Fast, in-vacuum tape system

Enhances decay of interest

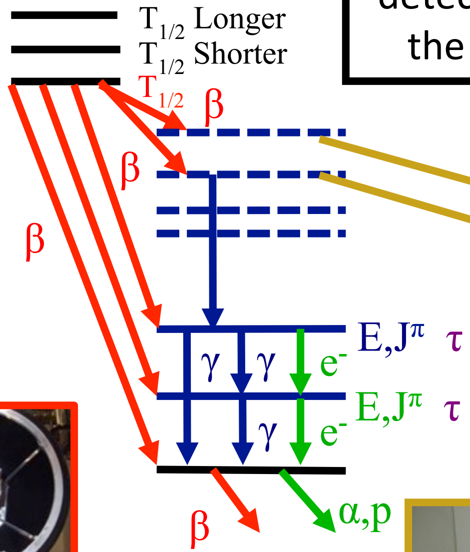

GRIFFIN reuses the full suite of ancillary detectors developed for the 8π spectrometer

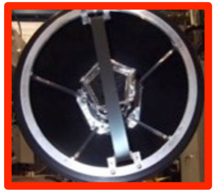

SCEPTAR: 10+10 plastic scintillators

Detects beta decays and determines branching ratios

DESCANT Neutron array

Detects neutrons to measure beta-delayed neutron branching ratios

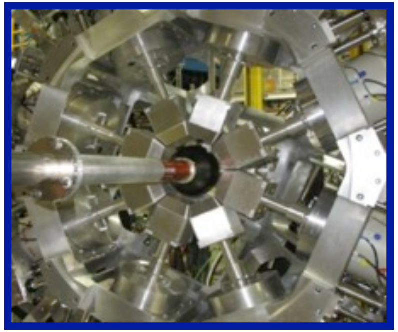

HPGe: 16 Clovers

Detect gamma rays and determines branching ratios, multipolarities and mixing ratios

LaBr$_3$: 8 LaBr$_3$

Fast-timing of photons to measure level lifetimes

Zero-Degree Fast scintillator

Fast-timing signal for betas

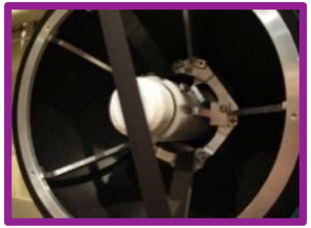

PACES: 5 Cooled Si(Li)s

Detects Internal Conversion Electrons and alphas/protons

GRIFFIN HPGe Clover Detectors

A close-packed array of 16 large-volume HPGe Clover detectors, 64 crystals

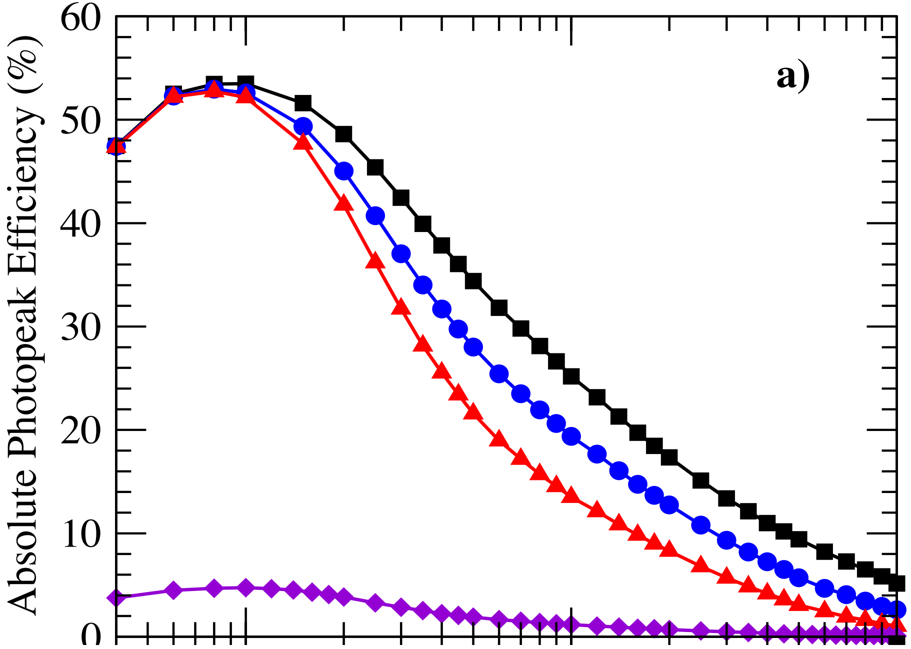

4096 crystal pairs at 52 unique angles for γ-γ angular correlations

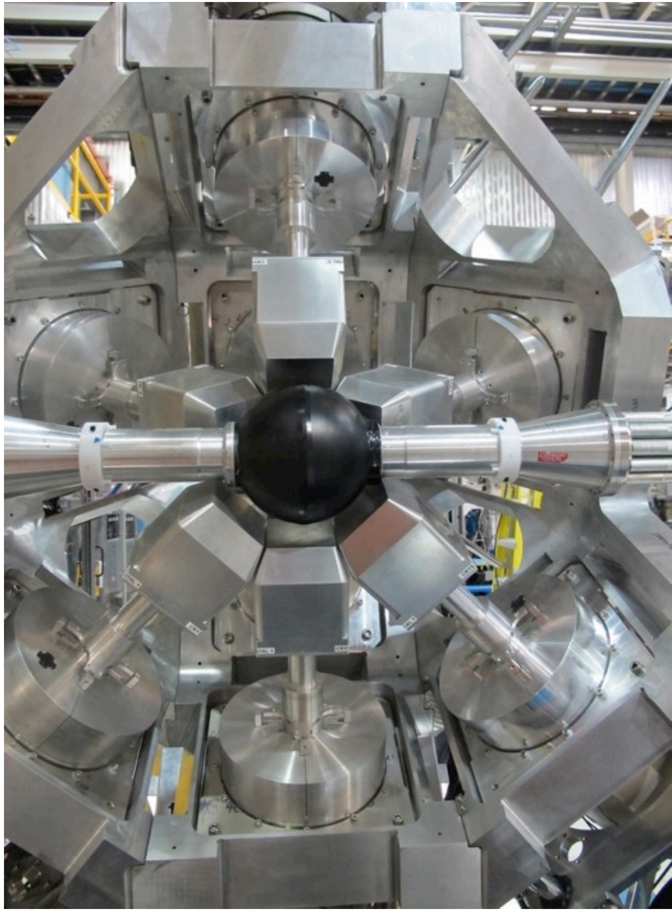

Gamma-Gamma Angular Correlation Analysis

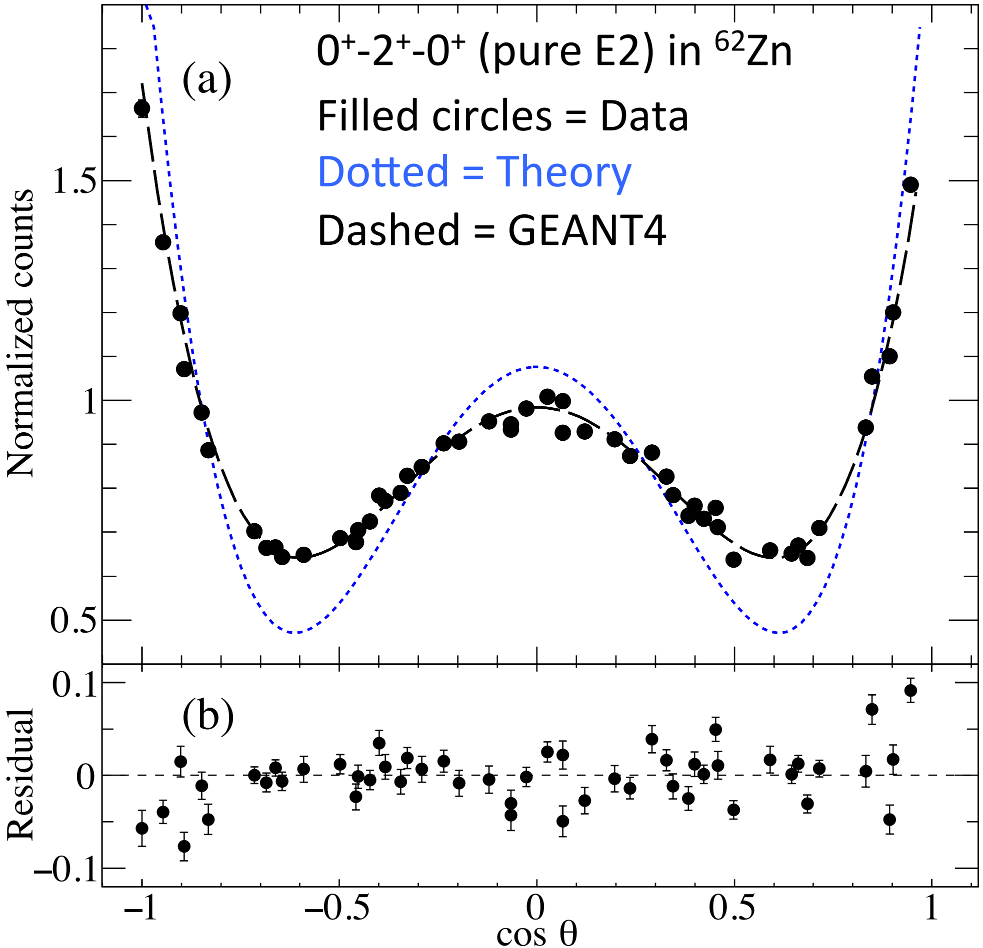

J.K. Smith, A.C. MacLean *et al. In preparation for NIM A (2017).*

Development of γ−γ angular correlation analysis techniques with GRIFFIN.

- Finite size and shape of crystals means theoretical distribution is attenuated.
- Obtain 'template' from high-statistics GEANT4 simulation
- Fit template to experimental data.

Ideally:

- Fit experimental data
- Plug coefficients into simple equations
- Obtain corrected 'true' coefficients

TRIUMF

GRIFFIN Results: Spectroscopy of ^{50}Sc and *ab initio* calculations of *B(M3)* strengths

A.B. Garnsworthy, M. Bowry, B. Olaizola, J.D. Holt, S.R. Stroberg *et al.*, Accepted to PRC (Oct 2017).
http://arxiv.org/abs/1710.06338

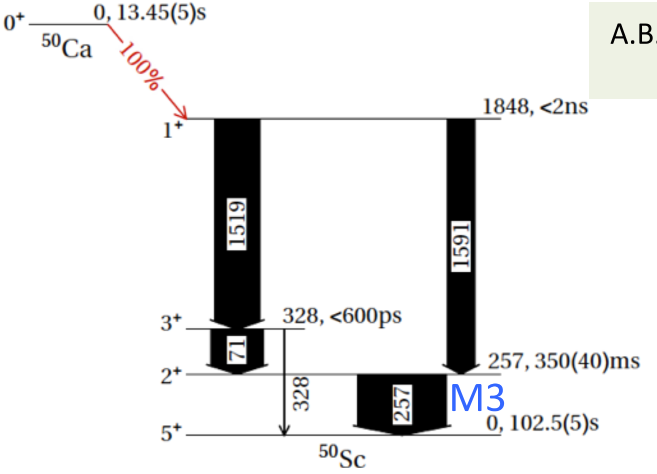

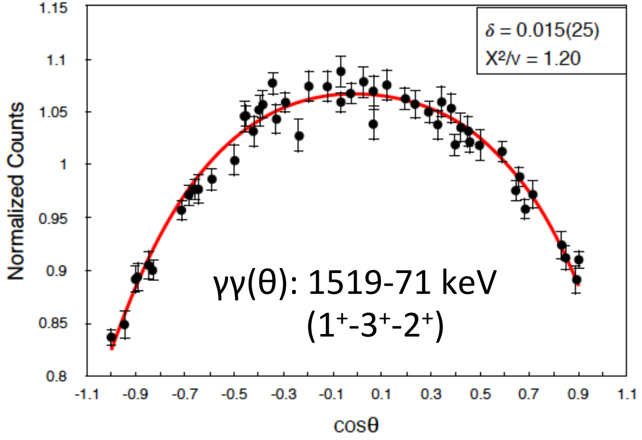

Gamma-gamma angular correlations with GRIFFIN confirm *M3* isomer in ^{50}Sc.

Isotope	E_γ (keV)	$J_i^\pi \to J_f^\pi$	ΔT	$T_{1/2}$	I_γ	α_{Tot}	I_{Tot}	Exp. $B(M3)$
^{24}Na [46–49]	472.2074(8)	$1^+ \to 4^+$	0	20.18(10)ms	0.9995(5)	0.000469(7)	0.9995(5)	9.10(7)
^{24}Al [50]	425.8(1)	$4^+ \to 1^+$	0	131.3(25)ms	0.83(3)	0.001144(16)	0.83(3)	2.4(6)
^{34}Cl [51]	146.36(3)	$3^+ \to 0^+$	1	31.99(3)min	0.383(5)	0.1656(24)	0.446(6)	0.10(1)
^{38}Cl [48, 52, 53]	671.365(8)	$5^- \to 2^-$	0	715(3)ms	0.3826(8)	0.000599(9)	1	0.0118(8)
^{38}K [54]	130.1(2)	$0^+ \to 3^+$	1	924.33(27)ms	$8(1)\times10^{-6}$	0.394(7)	0.00033(4)	0.29(10)
^{50}Sc [33]	257.895(1)	$2^+ \to 5^+$	0	350(40)ms	0.97(3)	0.0350(5)	0.99(1)	13.6(7)

First calculation of *B(M3)* strengths using *ab initio* Valence-Space In-Medium Similarity Renormalization Group method and effective operator.

Isotope	$J_i^\pi \to J_f^\pi$	ΔT	Exp. $B(M3)$	Phenomenological shell model $B(M3)$	VS-IMSRG Effective Op.
^{24}Na	$1^+ \to 4^+$	0	9.10(7)	19.9	4.45
^{24}Al	$4^+ \to 1^+$	0	2.4(6)	2.72	1.76
^{34}Cl	$3^+ \to 0^+$	1	0.10(1)	0.157	0.0013
^{38}Cl	$5^- \to 2^-$	0	0.0118(8)	0.0003	0.022
^{38}K	$0^+ \to 3^+$	1	0.29(10)	0.324	0.015
^{50}Sc	$2^+ \to 5^+$	0	13.6(7)	13.9	9.62

Compton Polarimetry using GRIFFIN

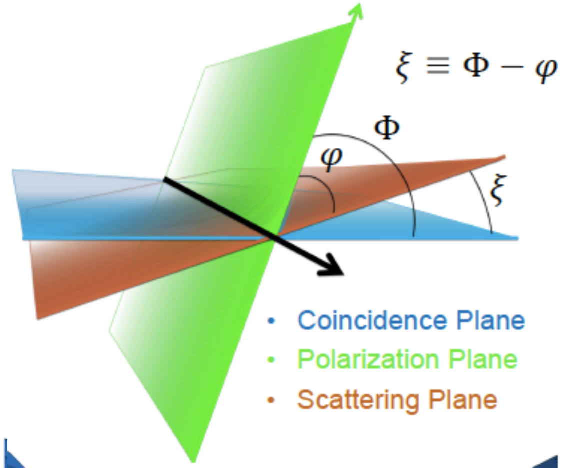

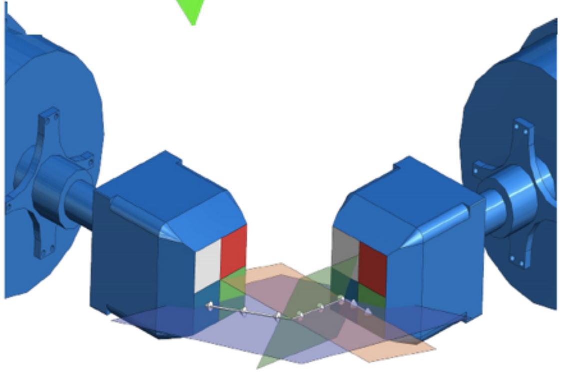

Define Polarization plane from γ–γ coincidence detection. Then examine azimuthal scattering angle to determine electric or magnetic nature of the radiation.

^{207}Bi Example: Red=567keV *E2*
Blue=1064keV *M4+E5*, δ_1=+0.03

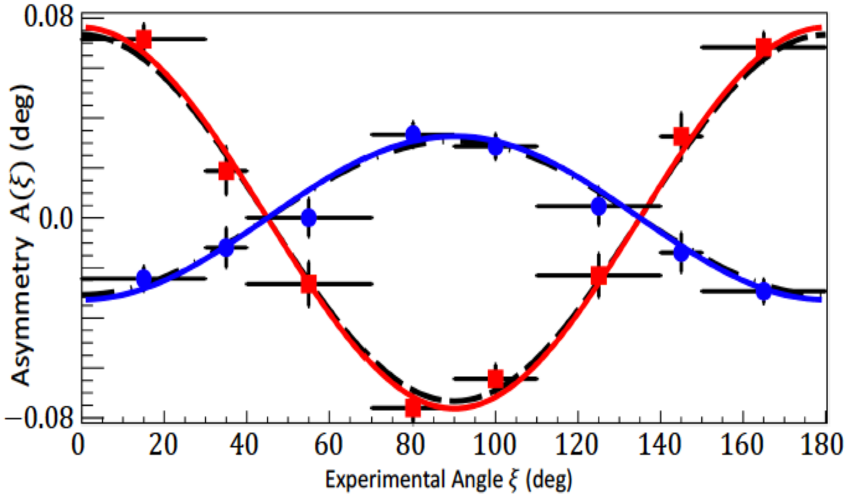

Dan Southall, TRIUMF research student, 2016

SCEPTAR - SCintillating Electron-Positron Tagging ARray

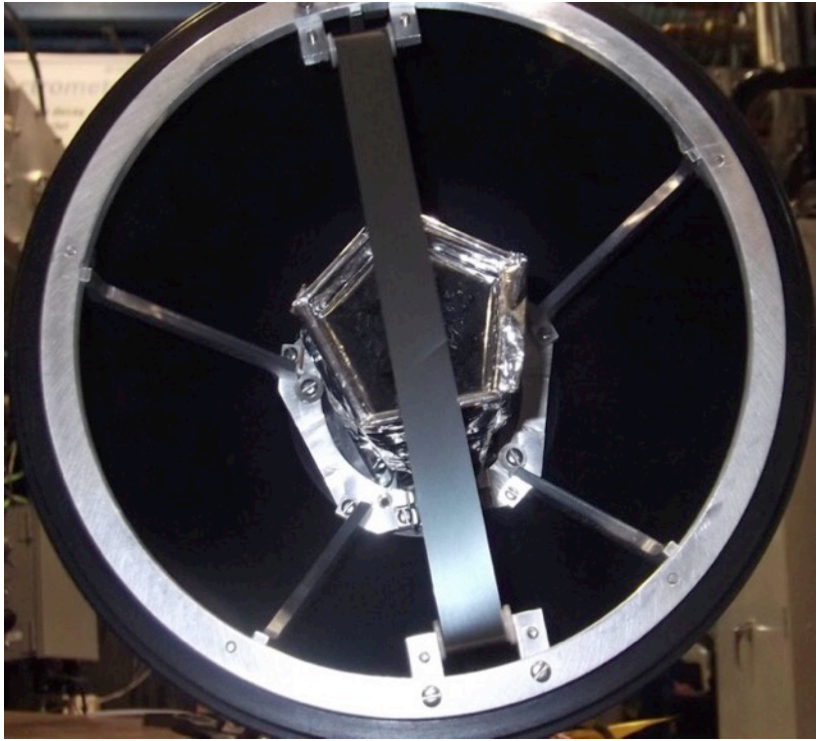

- Two hemispheres of 10 plastic scintillators
- Detects beta particles with ~80% solid angle coverage
- Improves peak-to-background of HPGe spectra

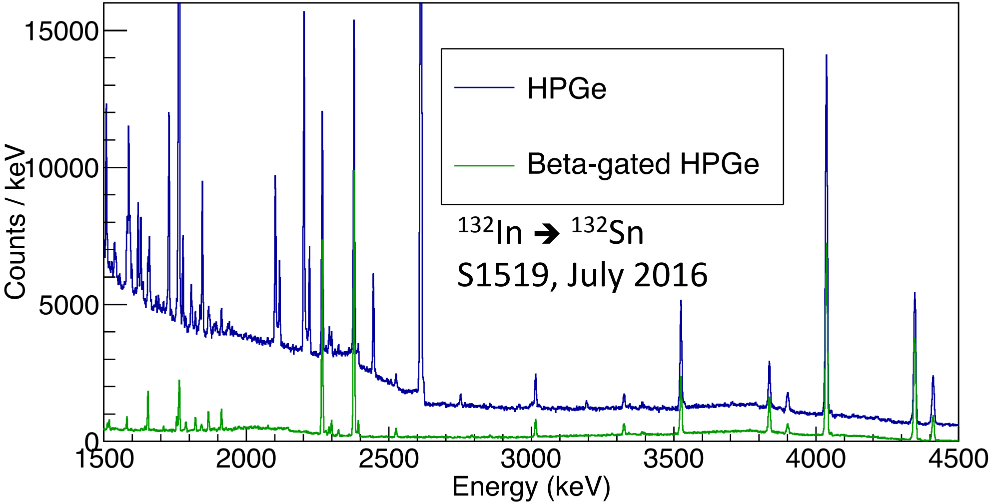

PACES - Pentagonal Array for Conversion Electron

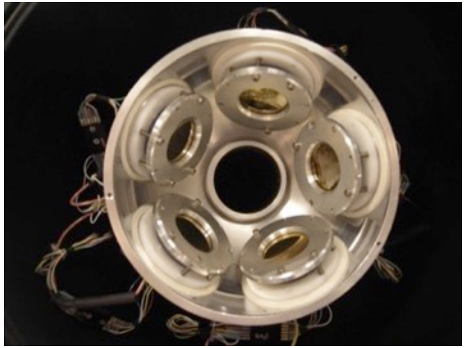

Five 5mm thick, 200mm^2 Si(Li), LN_2-cooled Si diode and FET

Solid angle coverage: 1.4% each, 7% total

~2keV resolution for electrons

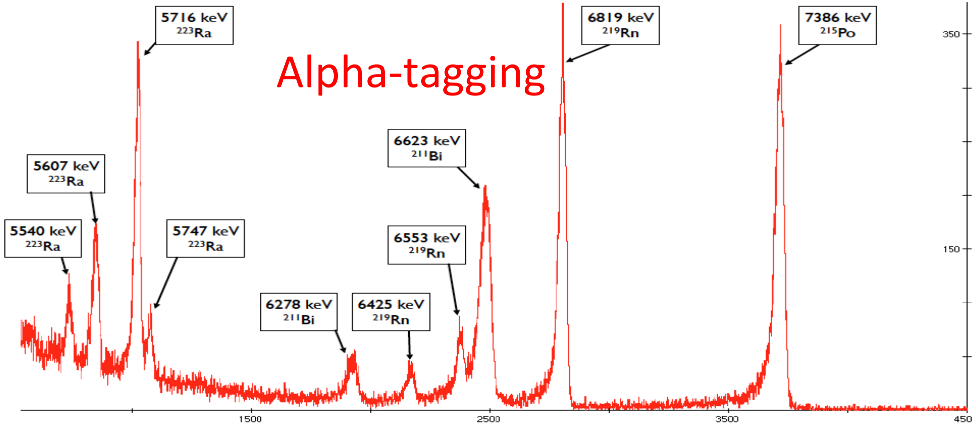

J. Park *et al.*, PRC 96, 014315 (2016).

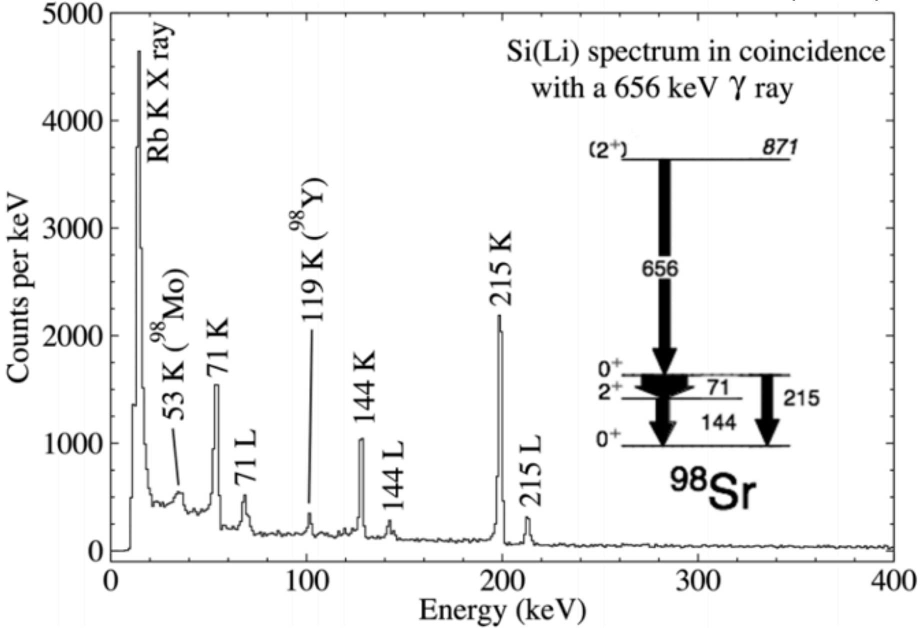

Gamma-Electron Angular correlations

Angular Correlation 975.7(e_K) – 569.7(γ)

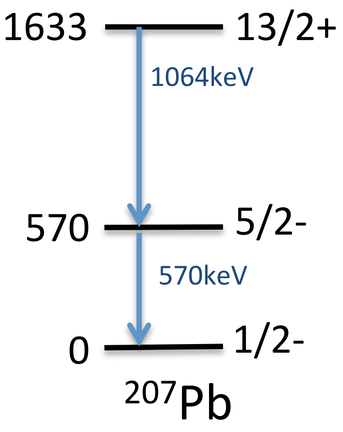

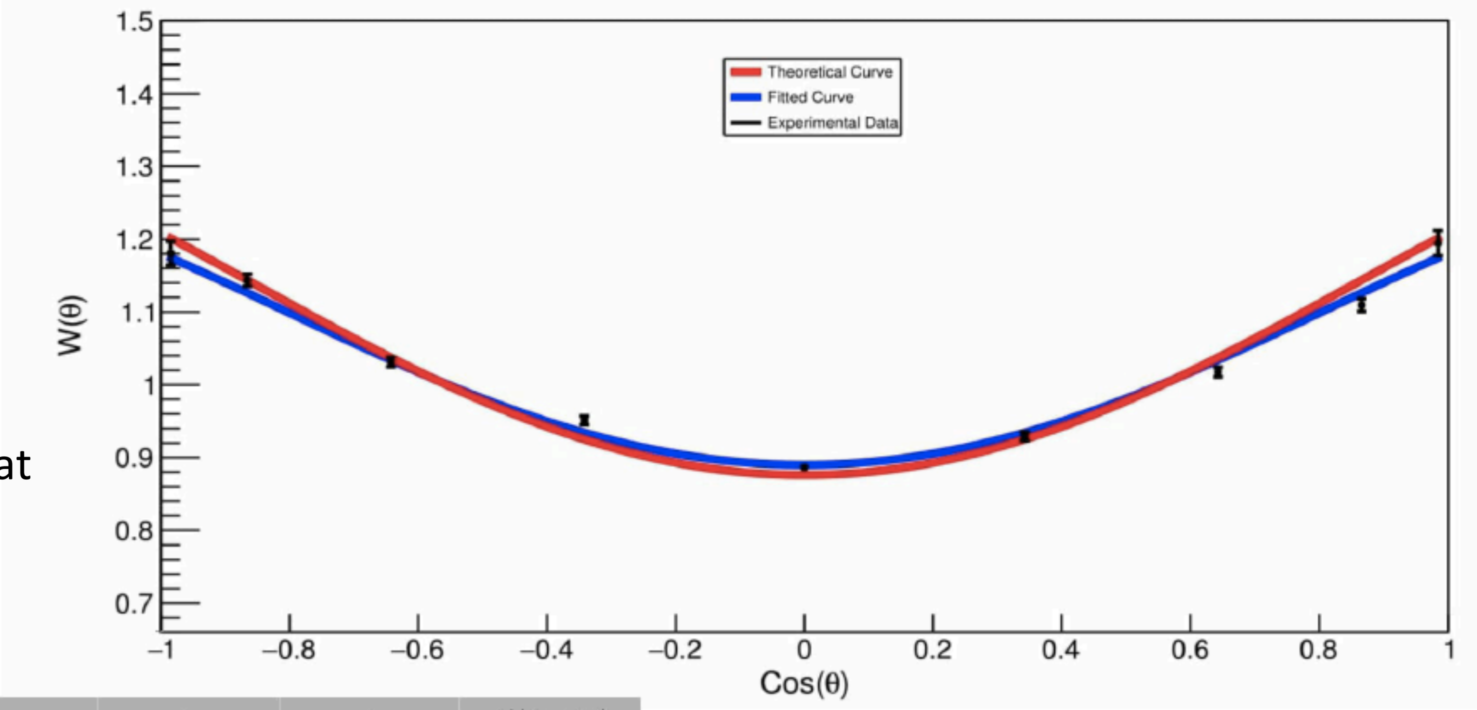

300 Ge-Si(Li) pairs at 18 unique angles for γ-e$^-$ angular correlations

	a_2	a_4	Chi Squared
Theory	0.231156	-0.022765	N/A
Experimental	0.202955	-0.022765	7.481581

TRIUMF $LaBr_3$ Fast-Scintillator Array for Excited-State Lifetime

- Eight $LaBr_3$(Ce) 2”x2” cylindrical crystal
- Source-detector distance=12.5 cm.
- GEANT4 simulated efficiency 1.4%@1.3MeV

- Hybrid analogue + digital electronics, excellent time resolution
- Effort led by Bruno Olaizola

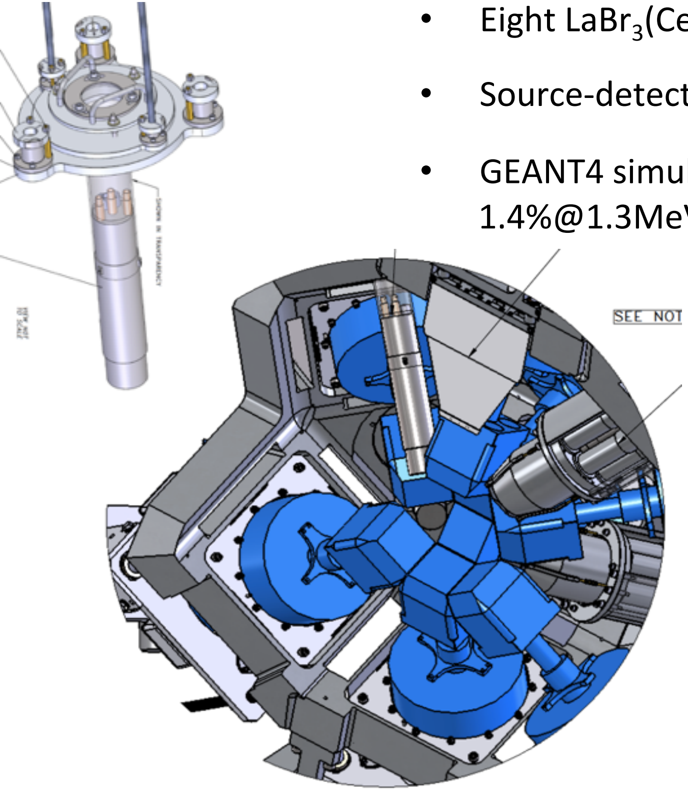

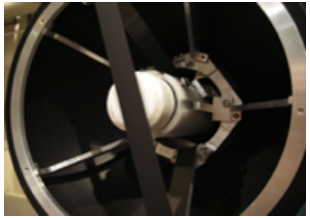

^{146}Cs β decay: GRIFFIN +DESCANT +$LaBr_3$

August 2016

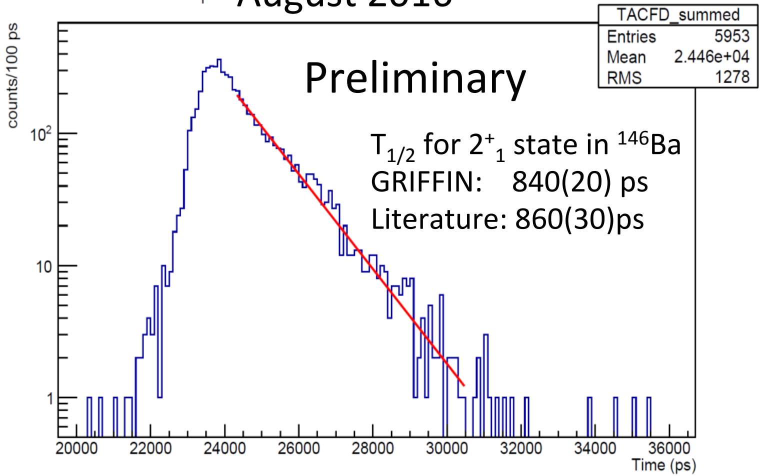

The GRIFFIN Spectrometer for precision decay studies at ISAC

TRIUMF

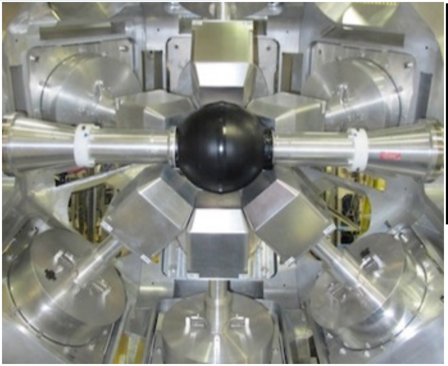

GRIFFIN is a powerful decay spectrometer for nuclear structure, astrophysics and fundamental interaction studies. Commissioned Fall 2014.

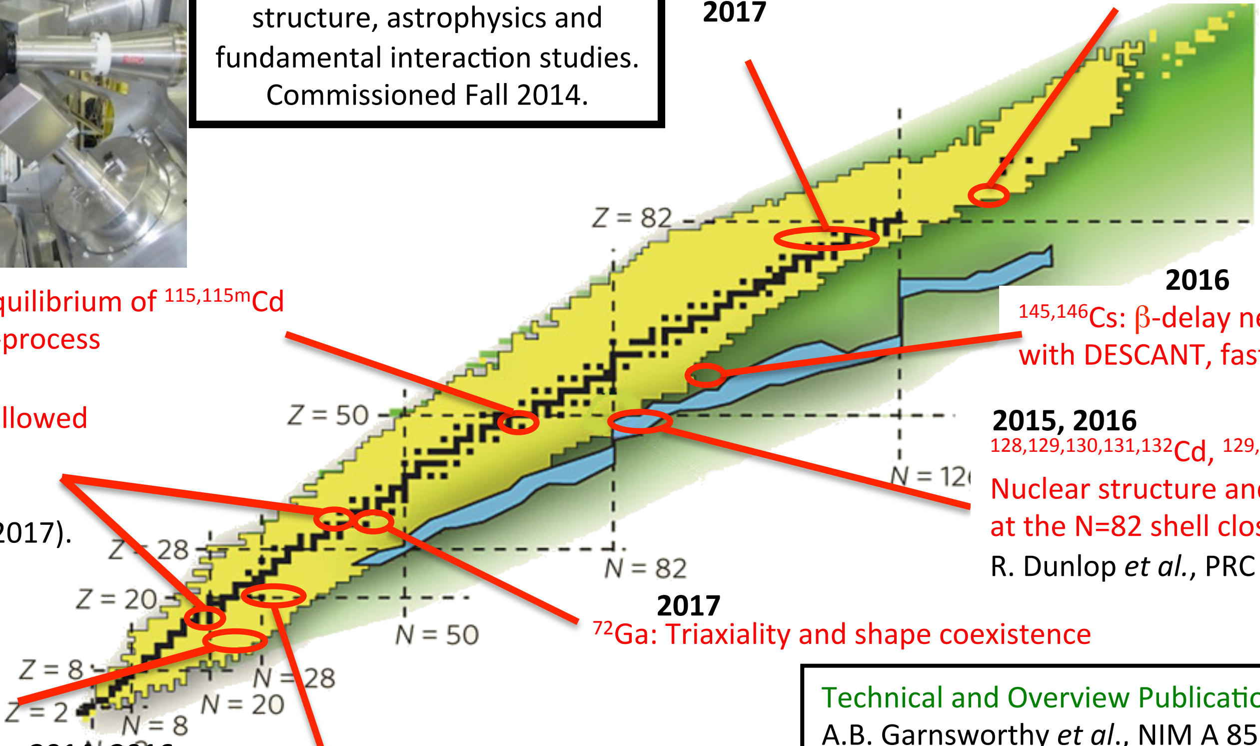

$^{188\text{-}200}$Tl: Development of collectivity in Hg isotopes **2017**

^{228,230}Fr: Probing Octupole deformation and collectivity in Radium isotopes. **2017**

Calibrations and development with ^{9}Li, ^{26}Na, ^{66}Ga beams

2014 ^{115,115m}Ag: Equilibrium of ^{115,115m}Cd during the s-process

2016 ^{145,146}Cs: β-delay neutron measurements with DESCANT, fast-timing with $LaBr_3$

2016
^{22}Mg, ^{62}Ga: Superallowed Fermi beta decays
M.R. Dunlop *et al.*, Accepted to PRC (2017).

2015, 2016
^{128,129,130,131,132}Cd, ^{129,130,131,132,133}In: Nuclear structure and r-process nucleosynthesis at the N=82 shell closure
R. Dunlop *et al.*, PRC 93, 062801(R) (2016).

2017
^{72}Ga: Triaxiality and shape coexistence

2014, 2015
^{31,32}Na, ^{33,34,35}Mg: Island of inversion

2014, 2016
^{46,47}K, ^{50}Ca: Single-particle and pair states near doubly-magic ^{48}Ca
A.B. Garnsworthy *et al.*, Accepted to PRC (2017).

Technical and Overview Publications
A.B. Garnsworthy *et al.*, NIM A 853, 85 (2017).
U. Rizwan *et al.*, NIM A 820, 126 (2016).
A.B. Garnsworthy, Acta Phys.Pol. B, 47, 713 (2016).
C.E. Svensson and A.B. Garnsworthy, Hyp. Int. 225, 127 (2014).

GRIFFIN studies around doubly-magic ^{48}Ca

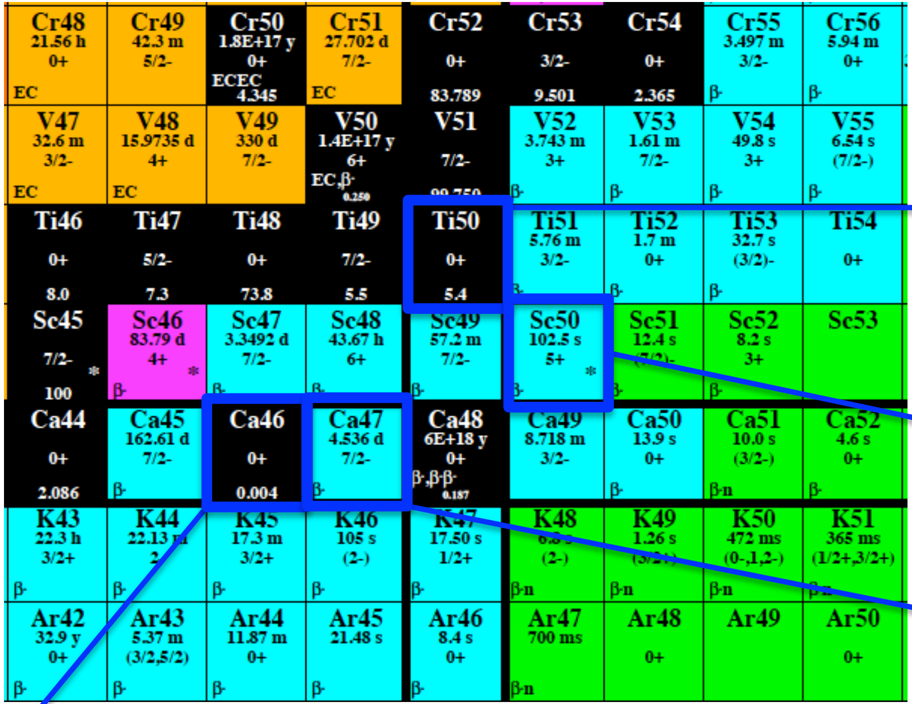

Two beamtime periods with GRIFFIN

- **1 publication accepted, 3 in preparation**
- **1 PhD thesis, 1 Masters thesis**

^{50}Sc - ^{50}Ti, Nov 2016, 1x10^6pps, ~8hrs
“Search for particle-hole excitations across the N=28 shell closure”, C. Jones, Masters thesis (2018).

^{50}Ca - ^{50}Sc, Nov 2016, 1x10^6pps, ~2hrs
“Spectroscopy of ^{50}Sc and the first calculation of *B(M3)* strengths using *ab initio* methods”, A.B. Garnsworthy, accepted in Phys. Rev. C (Oct 2017).

^{47}K – ^{47}Ca, Dec 2014, 1x10^5pps, ~90hrs
“Detailed decay spectroscopy of ^{47}Ca”, J.K. Smith, in preparation for Phys. Rev. C (2017).

^{46}K – ^{46}Ca, Dec 2014, 4x10^5pps, ~40hrs
“Detailed spectroscopy of ^{46}Ca: The investigation of the β decay of ^{46}K with the GRIFFIN γ-ray spectrometer”, J.L. Pore, PhD thesis (2017), in preparation for Phys. Rev. C (2017).

TRIUMF

^{46}K to ^{46}Ca Beta-Decay

^{46}K beam of 4×10^5 pps for ~40hrs

~200 gamma-ray transitions newly placed.

14 previously unobserved excited states (45 total observed).

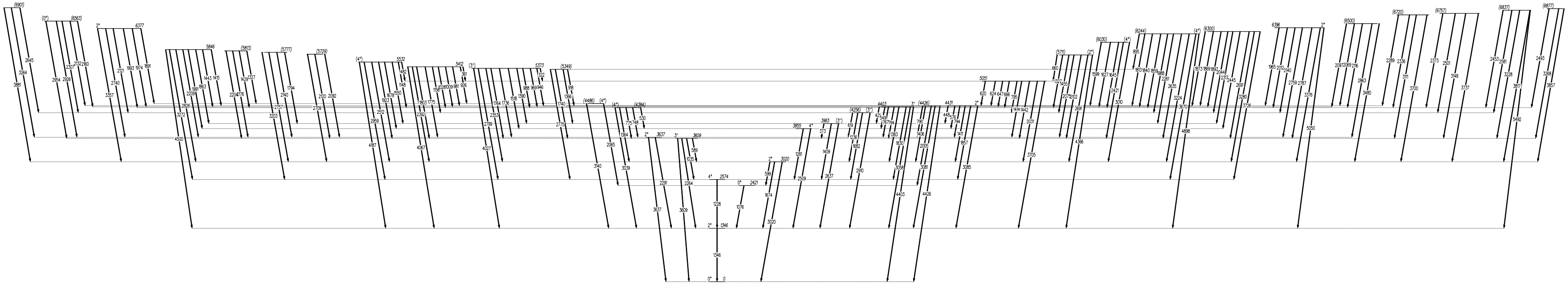

- States observed to within 815keV of the 7.7MeV Q value.
- Branching ratios observed down to 10^{-3}.
- Weakest γ-ray observed has intensity of 0.0015% that of the 2_1^+ to 0_1^+ transition.

- PhD thesis of J. Pore, Simon Fraser University.
- In preparation for PRC.

^{50}Sc – ^{50}Ti Search for p-n excitations across *N*=28 gap

Rowanwood Sect. 2.6 Fig. 2.6.5 v.7/26/16

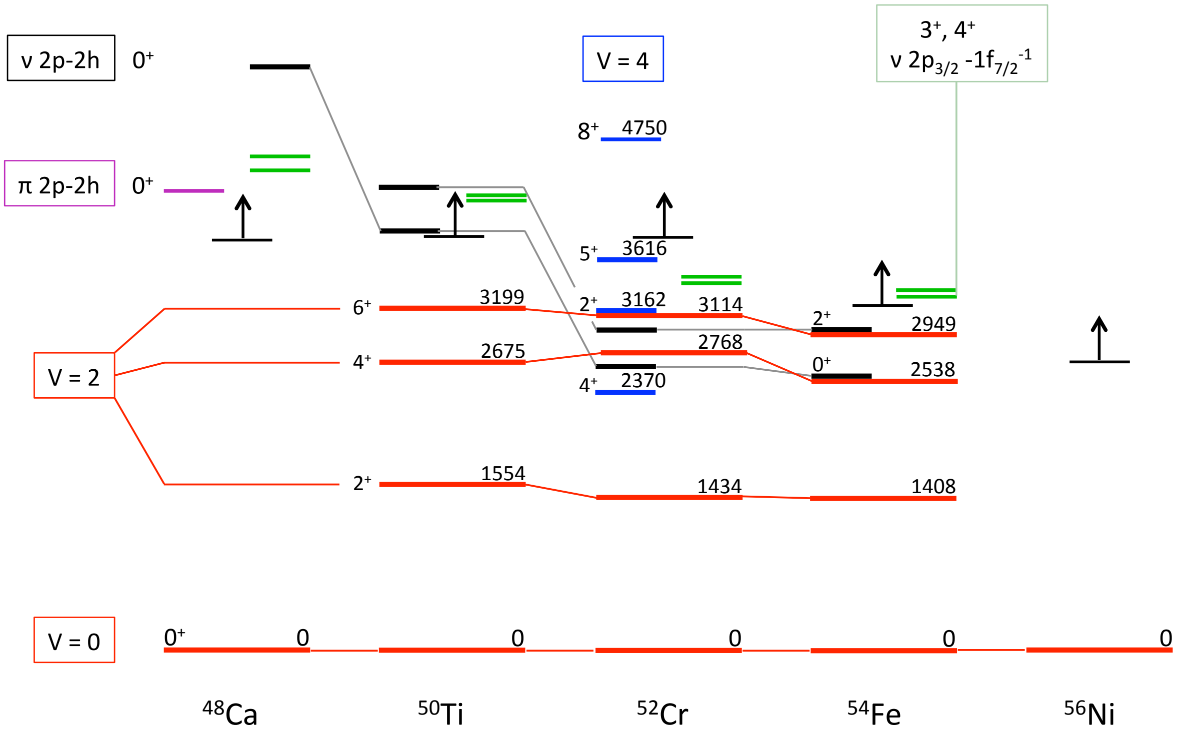

Seniority structures for the N = 28 isotones. The structure reflects the dominance of the $1f_{7/2}$ orbital. The v = 4 states are confined to ^{52}Cr. Note the order of the v = 2 and v = 4, $J^\pi = 4^+$ states in ^{52}Cr. Probable deformed structures due to the ν 2p-2h configuration are observed in ^{50}Ti, ^{52}Cr, ^{54}Fe. Selected ν 1p-1h states and the π 2p-2h in ^{48}Ca are shown. The vertical arrows indicate excitation energies above which other states are established.

^{50}Sc – ^{50}Ti Search for p-n excitations across *N*=28 gap

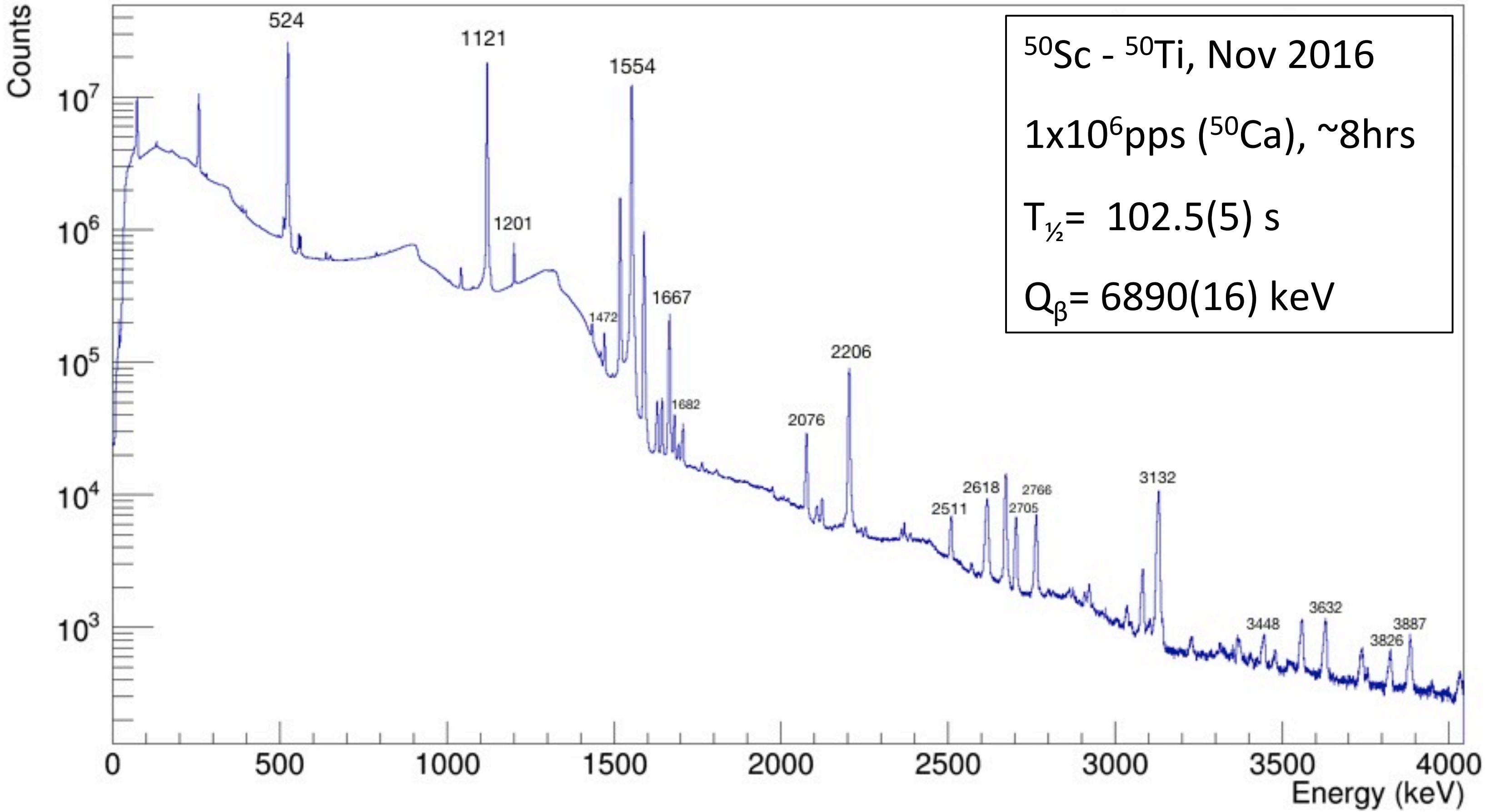

^{50}Sc - ^{50}Ti, Nov 2016

1x10^{6}pps (^{50}Ca), ~8hrs

$T_{½}$= 102.5(5) s

Q_{β}= 6890(16) keV

^{50}Sc – ^{50}Ti Search for p-n excitations across N=28 gap

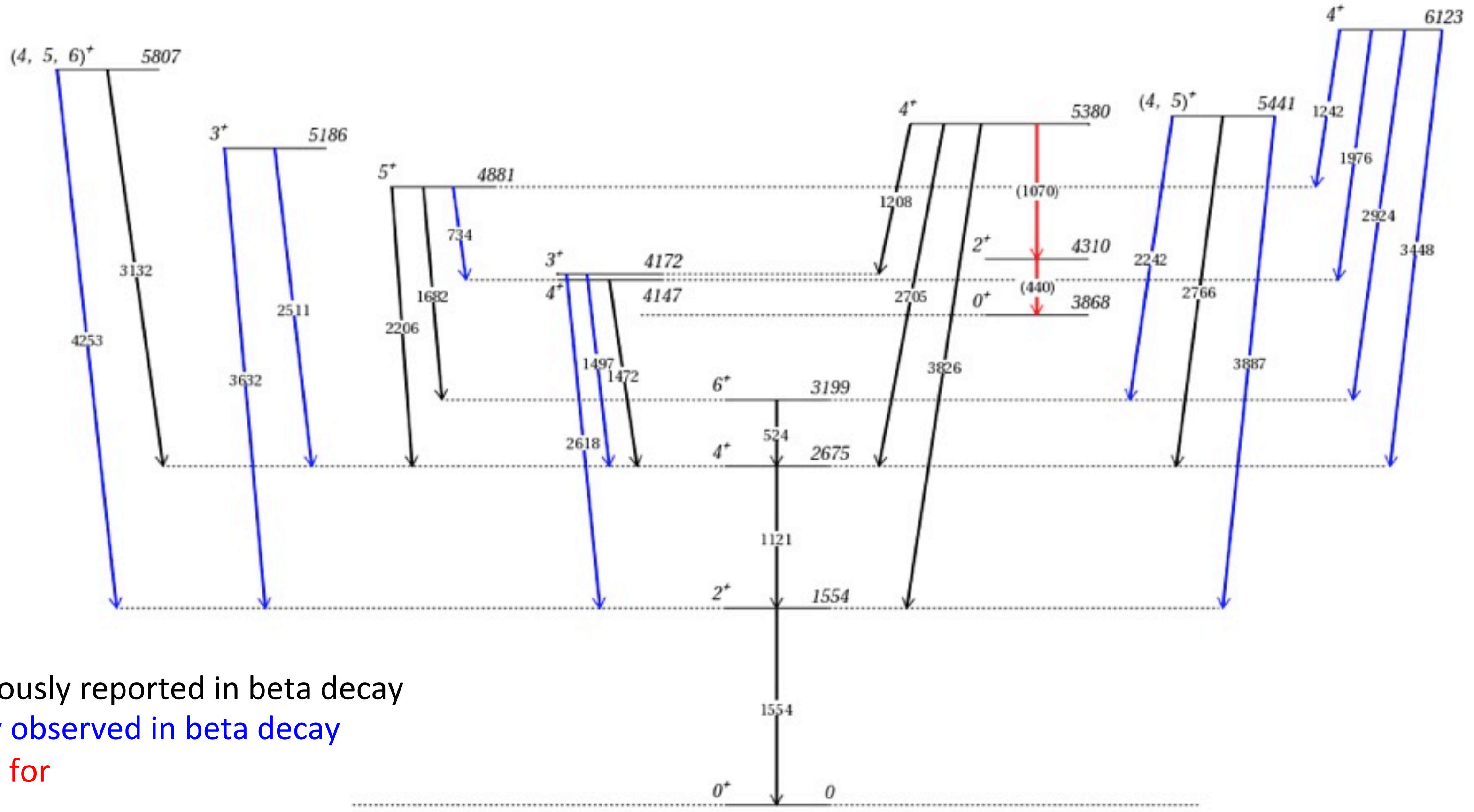

Black: Previously reported in beta decay

Blue: Newly observed in beta decay

Red: Search for

Hg isotopes from Tl decay

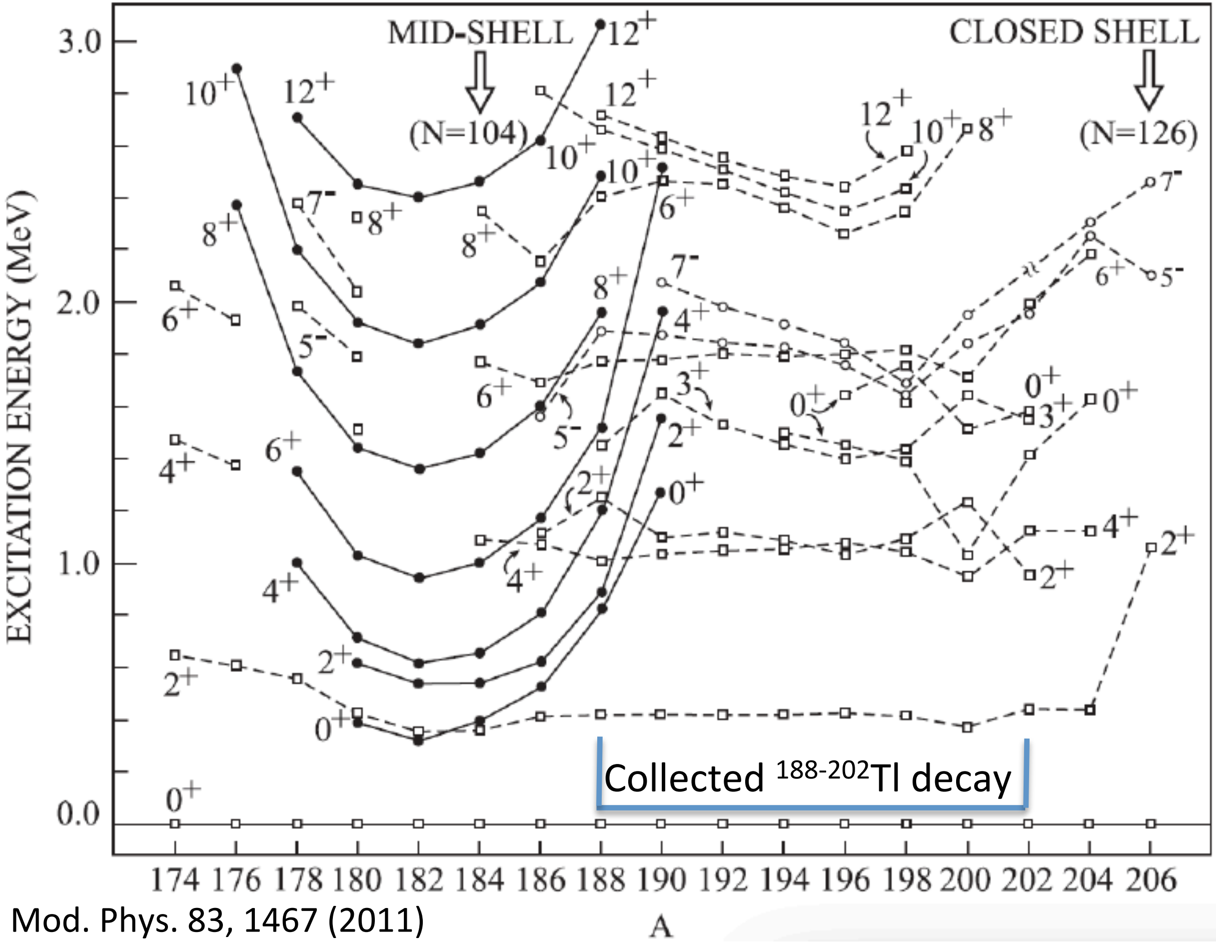

Collected $^{188-202}$Tl decay

Heyde & Wood, Rev. Mod. Phys. 83, 1467 (2011)

Hg isotopes from Tl decay

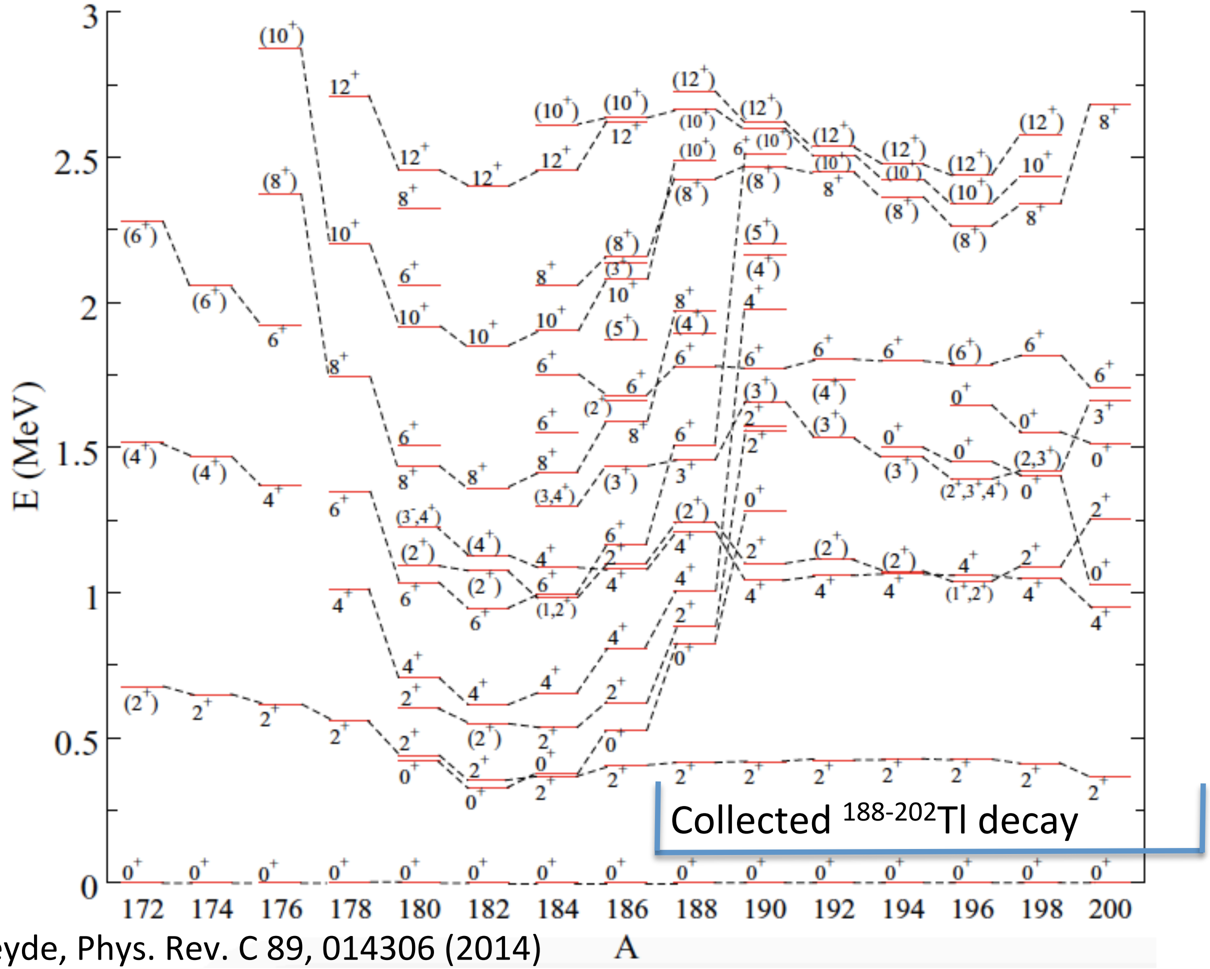

Garcia-Ramos & Heyde, Phys. Rev. C 89, 014306 (2014)

Hg isotopes from Tl decay

B.Olaizola, M. Bowry *et al.* TRIUMF
Beamtime April 2017

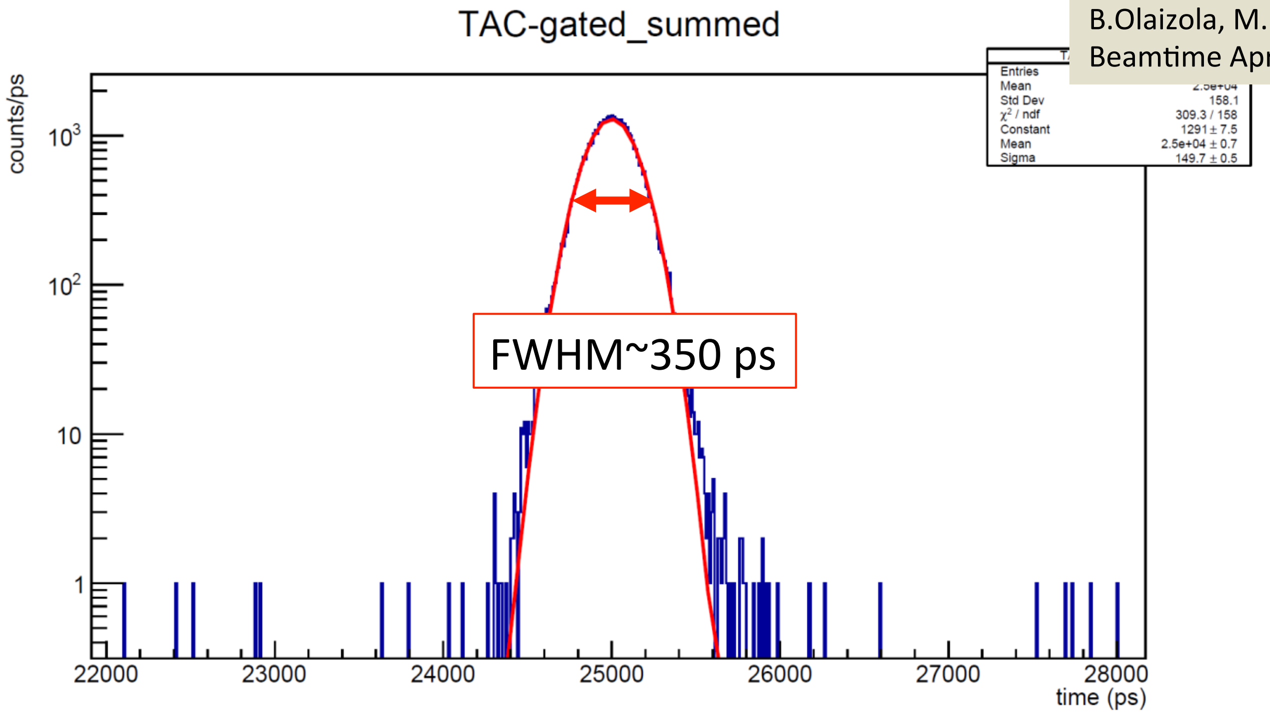

Timing resolution for Co-60 of the full array.
FWHM~350 ps, mainly for contributions of "bad" crystals
Good crystals down to FWHM~280 ps

Hg isotopes from Tl decay

B.Olaizola, M. Bowry *et al.* TRIUMF
Beamtime April 2017

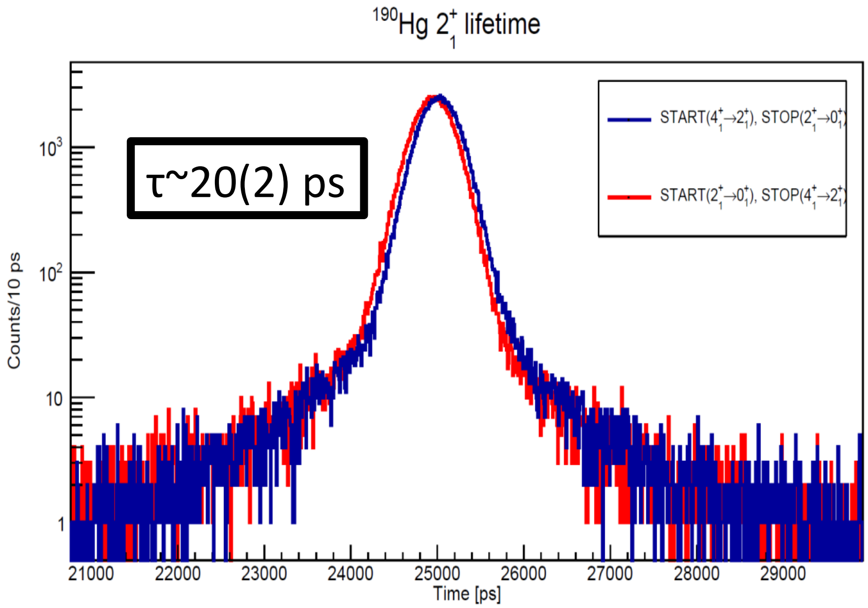

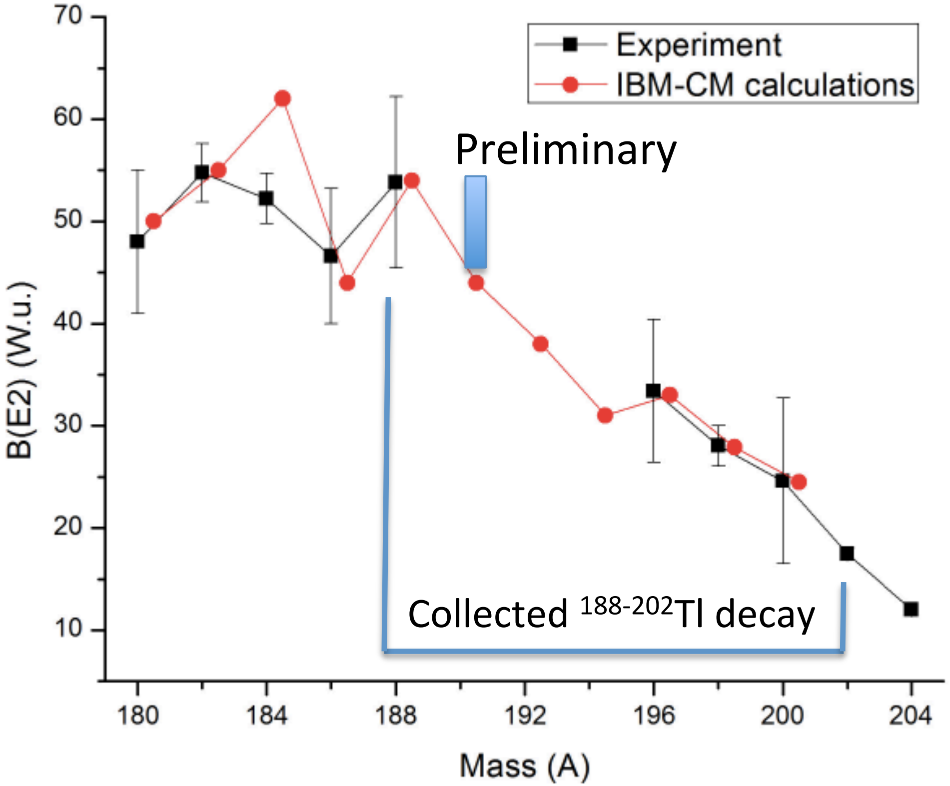

Detailed time-walk corrections need to be completed before results obtained for other isotopes

Even-mass Tl isomers

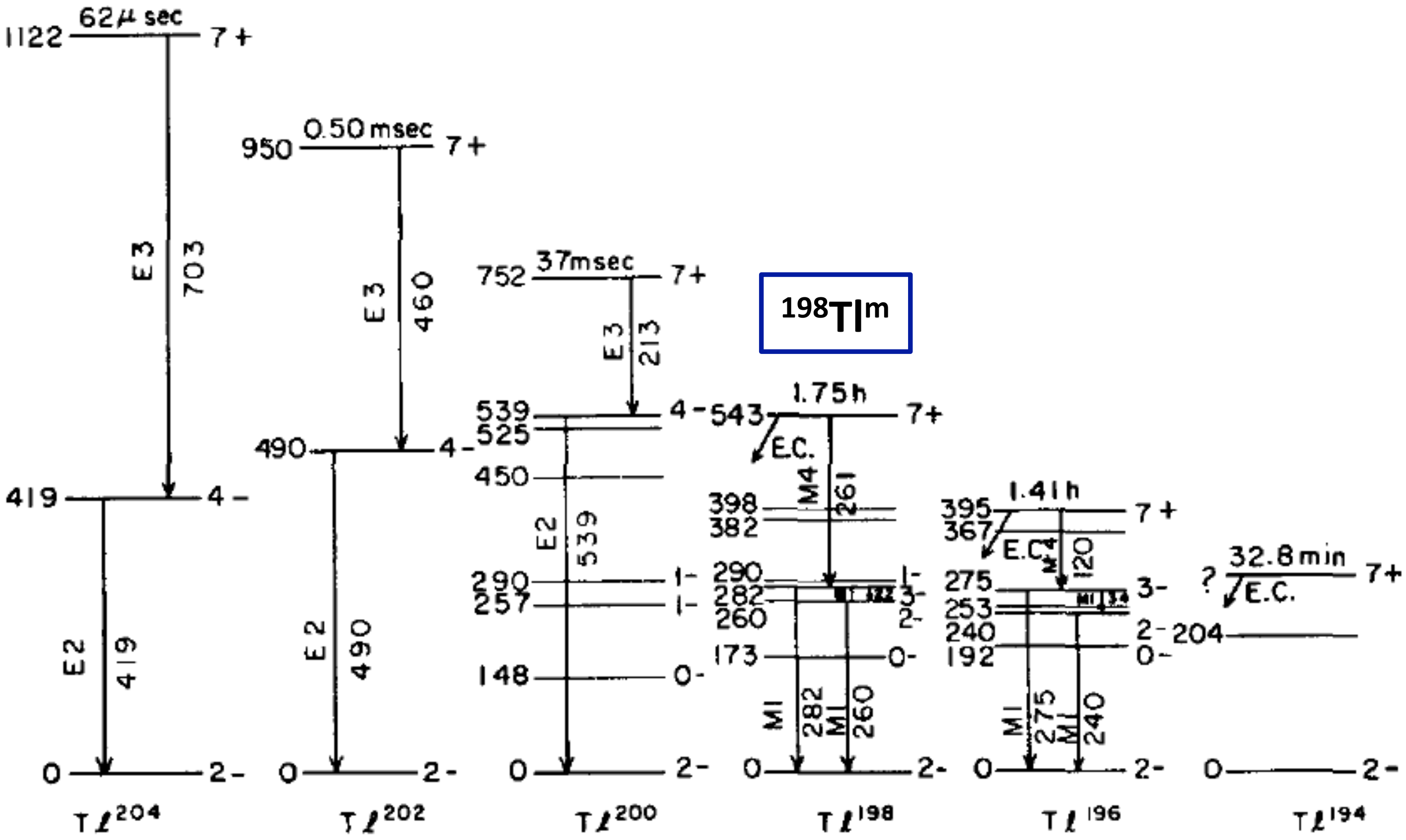

The nature of the excited states in the even-mass thallium isotopes is probably even more complicated than those of the odd-mass nuclei, and little can be said about them.

R.A. Diamond and F.S. Stephens, NPA 45, 632 (1963).

Electron spectroscopy of ^{198}Tl isomeric decay

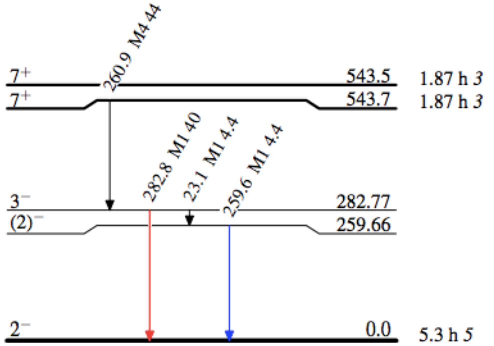

B.Olaizola, M. Bowry *et al.*
TRIUMF. Beamtime April 2017.

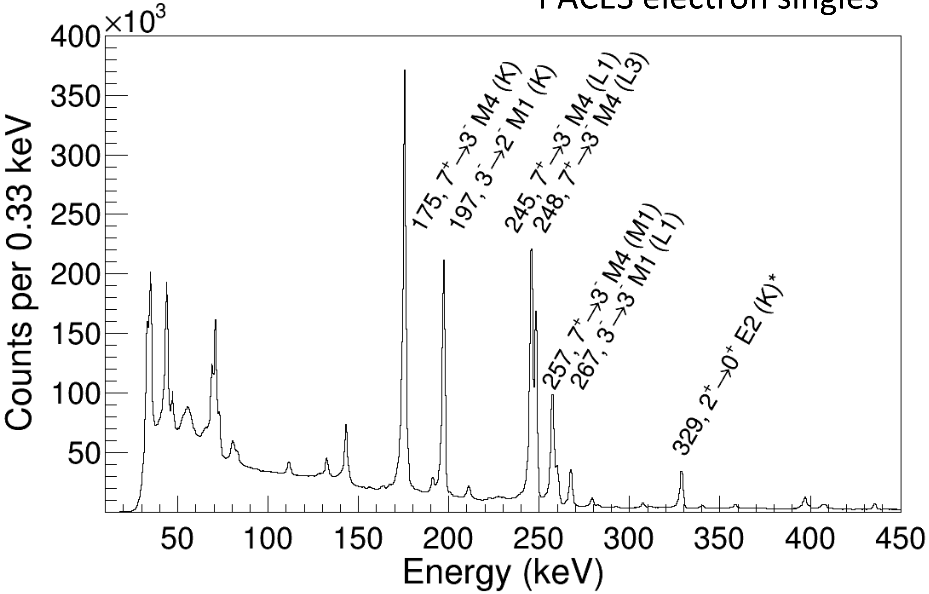

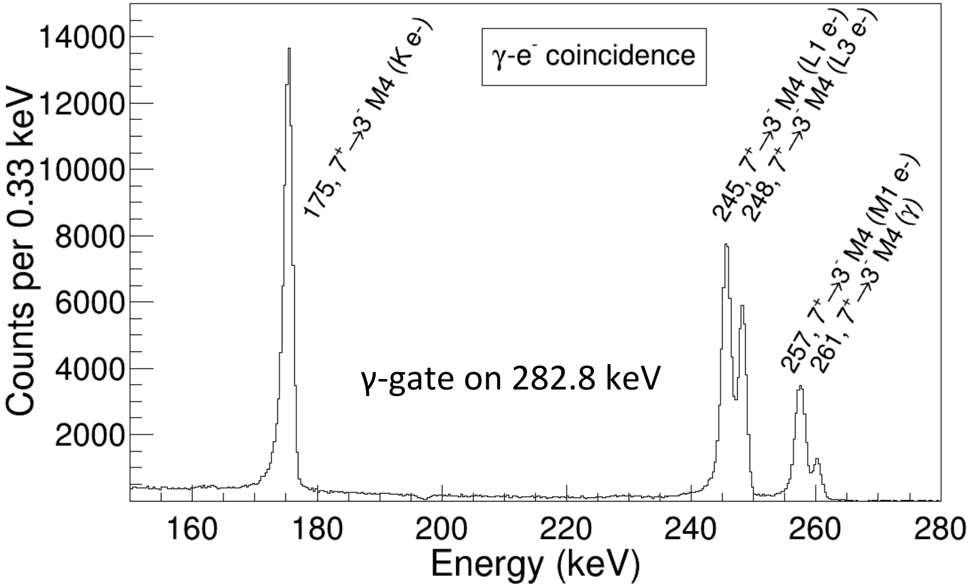

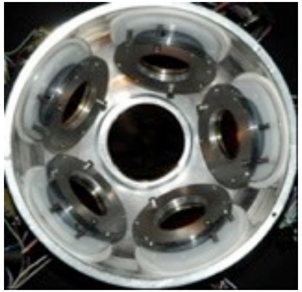

PACES array in GRIFFIN
Five 5mm thick, 200mm² Si(Li)

Electron spectroscopy of ^{198}Tl isomeric decay

B.Olaizola, M. Bowry *et al.* TRIUMF
Beamtime April 2017

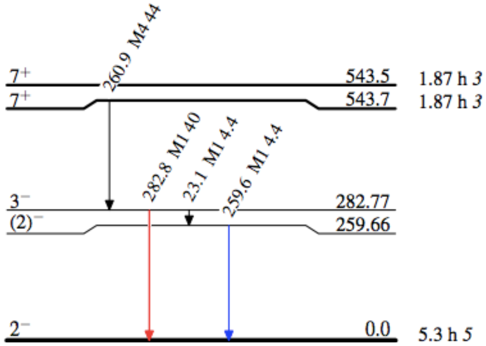

PACES array in GRIFFIN
Five 5mm thick, 200mm^2 Si(Li)

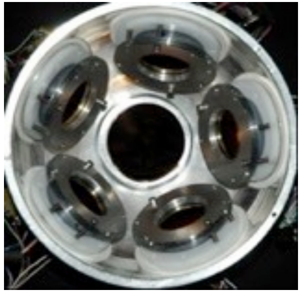

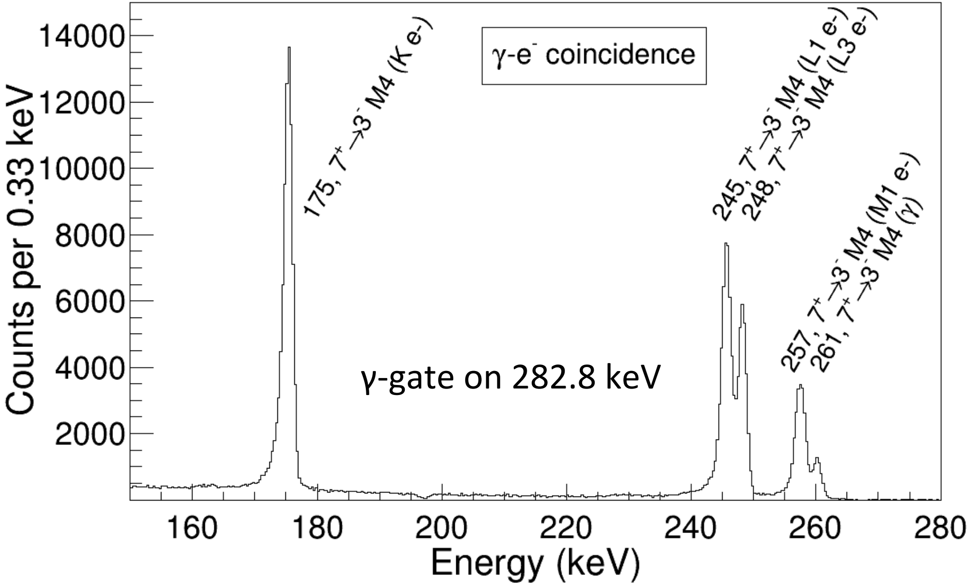

260keV Tl	Energy(keV)	M1	M4
Tot		0.581(9)	34.6(5)
K	174.47	0.476(7)	14.76(21)
L1	244.65	**0.0725(11)**	**6.55(10)**
L2	245.3	0.00738(11)	1.735(25)
L3	247.34	**0.000575(8)**	**6.1(9)**
L-tot	245.87	0.0805(12)	14.39(21)
K/L		5.91(12)	1.025(21)
M1	256.3	**0.01674(24)**	**1.76(25)**
M2	256.58	0.0019(3)	0.484(7)
M3	257.04	**0.000151(22)**	**1.82(3)**
M4	257.51	3.97(6)E-06	0.0399(6)
M5	257.61	2.83(4)E-06	0.034(5)
M-tot	256.68	0.0188(3)	4.14(6)
L/M		4.28(9)	3.47(7)

L1/L3

M1/M3

Structure of Ge isotopes

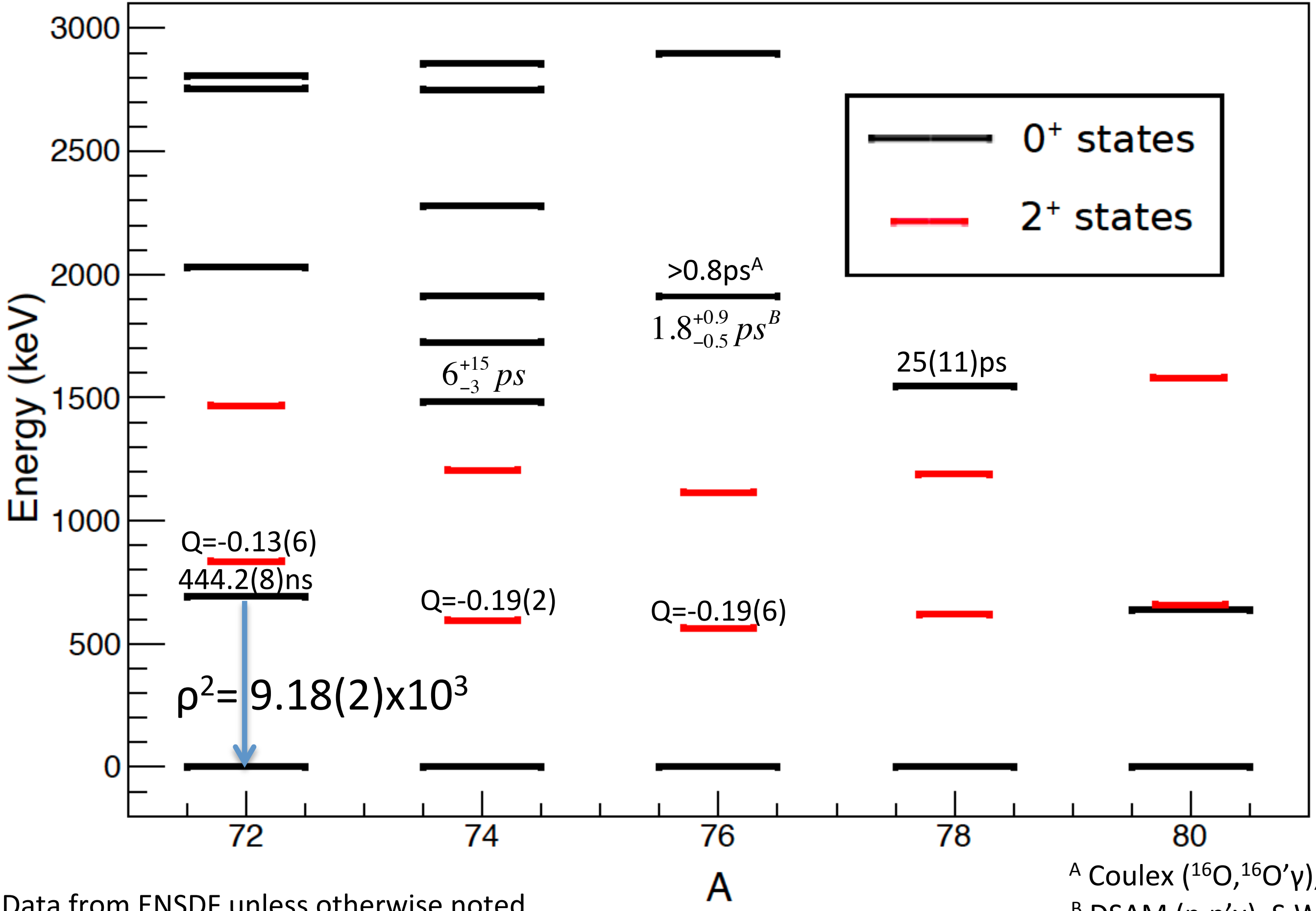

- Data from ENSDF unless otherwise noted.

[A] Coulex (^{16}O,$^{16}O'\gamma$), R.Lecomte et al., PRC 22, 2420 (1980).

[B] DSAM (n,n'γ), S.W. Yates, private communication (2016).

Ultra-high statistics beta-decay spectroscopy of ^{72}Ga-^{72}Ge

TRIUMF

A.B. Garnsworthy, J. Henderson, J. Smallcombe, J.K. Smith, M. Bowry, *et al.*, Beamtime Oct 2017

$T_{1/2}$=14 hours. Data collected for ~12 half lives.
The two GRIFFIN and PACES spectra below each represent 10GB out of a total of 8,000GB = 0.125%!

High Rate, ~3MBq, ~84µCi, 80MB/s total DAQ rate
16kHz Si(Li), 24kHz HPGe per channel

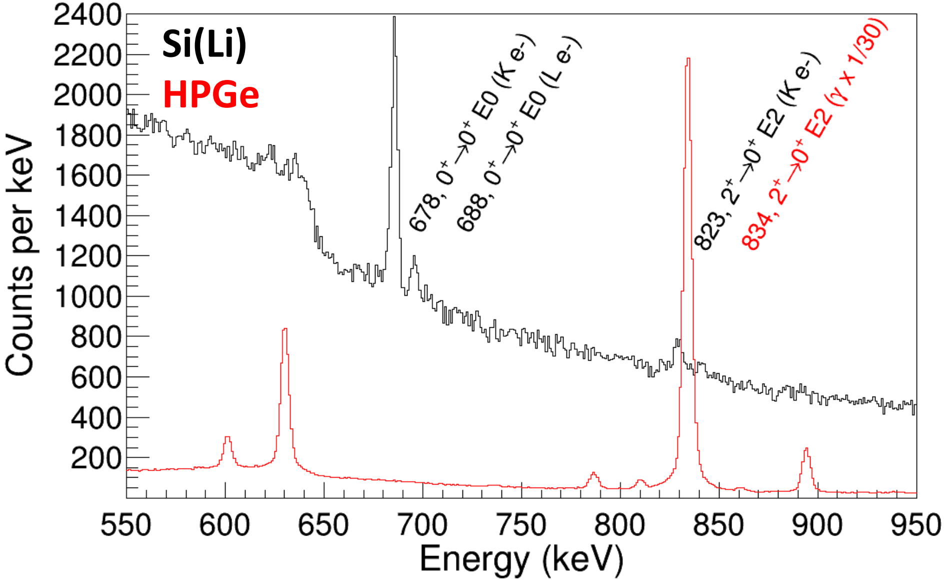

Low Rate, ~25kBq, ~0.7µCi, ~2MB/s total DAQ rate
0.5kHz Si(Li), 0.2kHz HPGe per channel

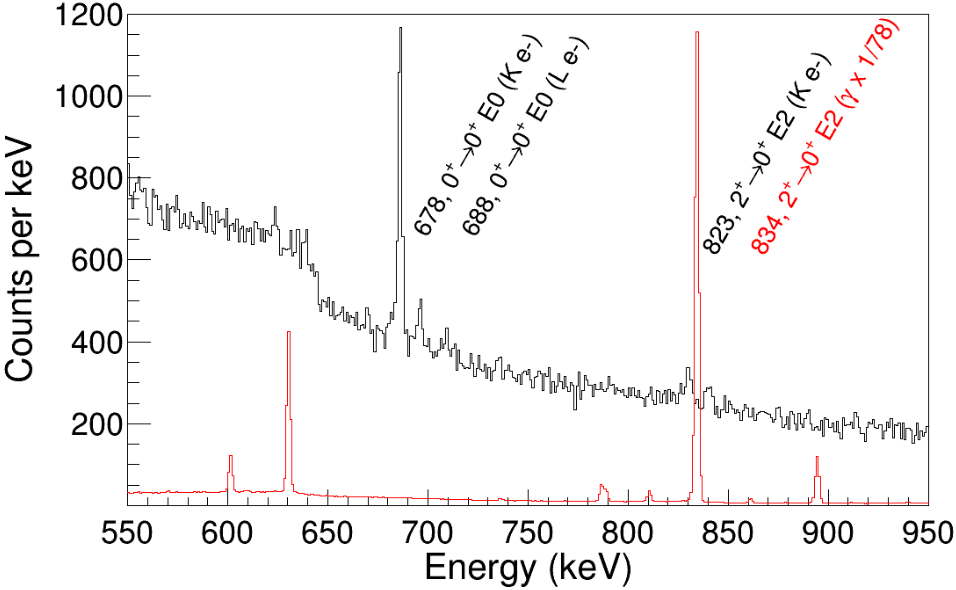

Questions and observations

- Identify benchmark cases for theory (*E0* strength):
  - ^{90}Zr = Doubly magic
  - ^{206}Pb, ^{68}Ni = valence neutrons
  - ^{26}Mg, ^{32}S & ^{58}Ni = valence protons and neutrons
  - Something = away from closed shells
- Standard sources for Internal conversion electron efficiency
- Lack of systematic information on behavior of ρ^2 values. No bench-marking of ‘normal’ values.

ICE calibration sources

133Ba	10.551 yrs				
	E (keV)		I (%)		ICC
	80.9971	12	34.11	28	1.703
	276.3997	13	7.147	30	0.0566
	302.851	6	18.3	6	0.0434
	356.0134	6	61.94	14	0.0254
	383.848	12	8.905	29	0.0202

207Bi	31.55 yrs				
	E (keV)		I (%)		ICC
	569.698	2	97.74	3	0.0217
	1063.656	3	74.5	2	0.128
	1770.228	9	6.87	4	0.0041

There is a very limited number of ICE calibration sources.

Often in-beam calibrations are done using the theoretical ICC of pure *E2* transitions.

TRIUMF

Potential long-lived ICE calibration sources

133Ba	10.551 yrs				
	E (keV)		I (%)		ICC
	80.9971	12	34.11	28	1.703
	276.3997	13	7.147	30	0.0566
	302.851	6	18.3	6	0.0434
	356.0134	6	61.94	14	0.0254
	383.848	12	8.905	29	0.0202

207Bi	31.55 yrs				
	E (keV)		I (%)		ICC
	569.698	2	97.74	3	0.0217
	1063.656	3	74.5	2	0.128
	1770.228	9	6.87	4	0.0041

182Ta	114.43 days				neutron capture on 181Ta (99%)
	E (keV)		I (%)		ICC
	100.10595	7	14.23	25	3.89
	152.42991	26	7.02	8	0.1258
	222.1085	3	7.57	8	0.048
	1121.29	3	35.3	2	-
	1189.04	3	16.42	10	0.0047
	1221.395	3	27.2	22	0.00305
	1231.004	3	11.57	8	0.00301

192Ir	73.831 days				neutron capture on 191Ir (37%)
	E (keV)		I (%)		ICC
	136.39	3	0.24	3	1.53
	295.95965	15	28.7	1	0.1047
	308.45507	17	29.8	1	0.0943
	316.50618	17	83	3	0.0841
	468.06885	26	47.7	2	0.0291
	588.581	7	4.49	2	0.01682
	604.41105	25	8.11	4	0.0258
	612.46215	26	5.28	3	0.01536

228Th	1.9131 yrs		Alpha decay + Daughter decays		
	E (keV)		I (%)		ICC
	84.4		1.22	2	21.2
	238.6		43.5	4	0.909
	241		4.1	5	0.276
	277.4		2.3	3	
	300.1		3.25	3	0.484
	510.8		8.18	10	
	583.187	2	30.6	2	
	727.3		6.69	9	0.0141
	860.6		4.5	4	
	1620.7		1.49	5	0.0064
	2614.511	10	35.86	6	

^{170}Lu 2days ^{171}Yb(p,2n) or ISOL

Microscopic model for *E0* transition matrix elements

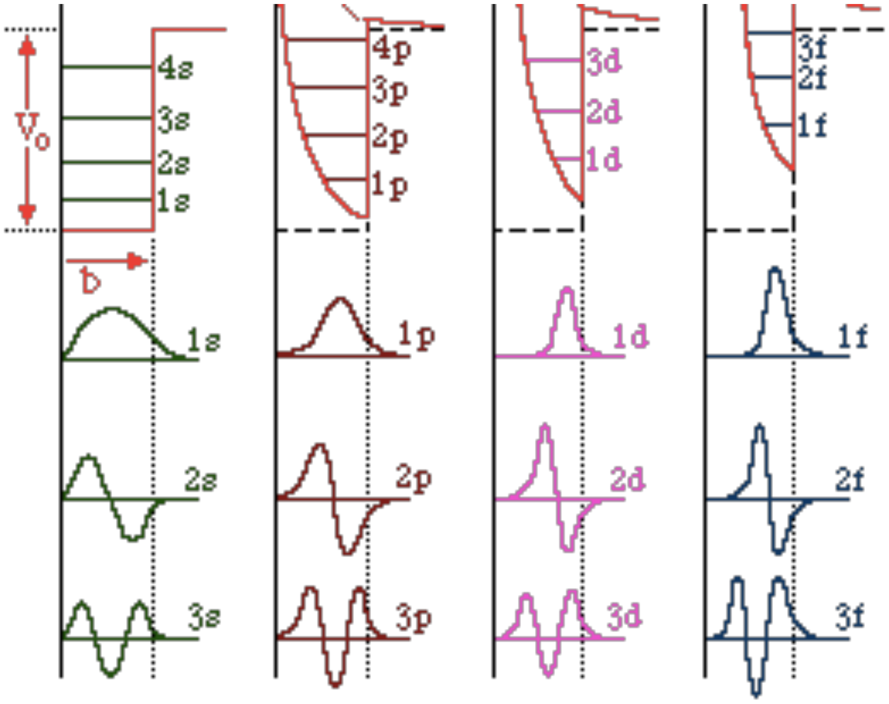

Radial wavefunctions R_{nl}

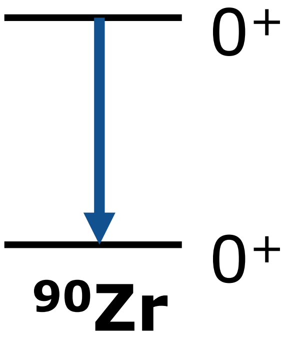

$1g_{9/2}$ and $2p_{1/2}$

SM: 4.71

MM: 0.71

Largest node changes on the chart:

N=60 ($1g_{7/2}$-$3s_{1/2}$) ^{98}Sr
N=104 ($3p_{3/2}$-$1i_{13/2}$) ^{186}Pb

Maybe expect the largest core-polarization effect in these regions (not necessarily the largest *E0* strength)